TOPICAL REVIEW — Magnetism, magnetic materials, and interdisciplinary research

Progress in bulk $MgCu_2$-type rare-earth iron magnetostrictive compounds*

Ren Wei-Jun(任卫军)† and Zhang Zhi-Dong(张志东)‡

Shenyang National Laboratory for Materials Science and International Centre for Materials Physics, Institute of Metal Research, Chinese Academy of Sciences, Shenyang 110016, *China*

(Received 18 May 2013)

Studies of bulk $MgCu_2$-type rare-earth iron compounds with Laves phase are reviewed. The relationship between magnetostriction and structural distortion and the consequent crystallographic method for measuring magnetostriction are introduced at first. Then we review recent progress in understanding bulk magnetostrictive Laves phase materials, especially the magnetostriction and the minimization of the anisotropy of the light rare-earth Pr- and Sm-based compounds. Finally, a summary and outlook for this kind of compounds are presented.

Keywords: magnetostriction, anisotropy, Laves compound

PACS: 75.80.+q, 75.50.Bb, 75.30.Gw **DOI:** 10.1088/1674-1056/22/7/077507

1. Introduction

As defined by the International Union of Pure and Applied Chemistry, rare-earth elements (or rare-earth metals) are a set of seventeen chemical elements in the periodic table, namely, the fifteen lanthanoids plus scandium and yttrium. Scandium and yttrium are considered rare-earth elements because they tend to occur in the same ore deposits as the lanthanoids and exhibit similar chemical properties. Most of the rare-earth elements possess 4f electrons, strong spin–orbit coupling, and large atomic moment. Their outstanding optical, magnetic, electrical characteristics motivate the many and varied applications of rare-earths in both civil and martial industries. Rare-earth magnetic materials now are in demand for applications including rare-earth permanent magnets such as $Nd_2Fe_{14}B$, $SmCo_5$, Sm_2Co_{17}, room-temperature (RT) magnetocaloric materials, for instance, Gd metal, and magnetostrictive materials, $TbFe_2$, $SmFe_2$, and $RR'Fe_2$ pseudobinary compounds (R and R' stand for different rare-earth elements). Here magnetostrictive materials refer to ferromagnetic/ferrimagnetic compounds that undergo a great deformation when the magnetization is changed either by a change in temperature or by the application of a magnetic field. The deformation itself is called magnetostriction. For example, cooling a paramagnetic state body into a ferromagnetic state produces a volume expansion. Alternatively, applying a magnetic field to a ferromagnetic/ferrimagnetic body induces a linear deformation. All magnetic materials exhibit magnetostriction to some degree; however, giant magnetostriction occurs only in a small number of materials, most of which contain rare-earth elements. The rare-earth magnetostrictive material $TbFe_2$ has the largest magnetostriction at RT.[1] Although rare-earth-free magnetostrictive materials Fe–Ga and Fe–Al have been found, they are sensitive to magnetic fields, but their magnetostriction is only about 10%–20% of the typical extent of a rare-earth material.[2] Some (Ni_2MnGa) of the Heusler alloys may exhibit strain even larger than that of rare-earth magnetostrictive materials when the magnetic field induces a martensite–austenite phase transition. The action is similar to that of magnetostriction, but the response is much slower and always irreversible. They can be taken as special magnetostrictive materials and only be used in static or quasistatic conditions, as has been reviewed by Söderberg *et al.* in 2006[3] and Trudel *et al.* in 2010[4]. Interest in rare-earth magnetostrictive materials has boomed since Darnell[5] and Legvold *et al.*[6] found large magnetostriction in pure rare-earth metals Tb and Dy. The extent of their magnetostriction is hundreds times of that of a transition metal. The fault of rare-earths in application is their low Curie temperature T_C. In the 1970s, Clark *et al.* found large magnetostriction in RFe_2 Laves compounds, and practical rare-earth magnetostrictive materials have been developed based on them.[7–9] This has been reviewed by Clark,[1] Koon *et al.*,[10] Andrev,[11] and Jiles.[12] In the present paper, we focus on progress with bulk RFe_2 magnetostrictive materials since the 1990s.

*Project supported by the National Basic Research Program of China (Grant No. 2012CB619404).

†Corresponding author. E-mail: wjren@imr.ac.cn

‡Corresponding author. E-mail: zdzhang@imr.ac.cn

© 2013 Chinese Physical Society and IOP Publishing Ltd

2. Structural distortion and measurement of *R*Fe$_2$-type magnetostrictive compounds

2.1. Structural distortion and magnetostriction of *R*Fe$_2$ magnetostrictive materials

As shown in Fig. 1, magnetostrictive compound *R*Fe$_2$ has a MgCu$_2$-type C15 Laves phase structure, which belongs to the cubic system above its T_C. A commonly accepted expression for the magnetostriction of cubic crystals has the form

$$\lambda = h_1\left(\alpha_1^2\beta_1^2+\alpha_2^2\beta_2^2+\alpha_3^2\beta_3^2-\frac{1}{3}\right) +2h_2(\alpha_1\alpha_2\beta_1\beta_2+\alpha_1\alpha_3\beta_1\beta_3+\alpha_3\alpha_2\beta_3\beta_2). \quad (1)$$

Here α_i denote the direction cosines of the magnetization with respect to the crystal axes, and β_i denote the direction cosines of the measurement direction with respect to the crystal axes. When both magnetization and measurement direction lie in the same direction [100], one may get the magnetostriction along [100]

$$\lambda_{100}=\frac{2}{3}h_1, \quad (\alpha_1=\beta_1=1, \quad \alpha_2=\beta_2=\alpha_3=\beta_3=0). \quad (2)$$

In the same way,

$$\lambda_{111}=\frac{2}{3}h_2, \quad (\alpha_1=\beta_1=\alpha_2=\beta_2=\alpha_3=\beta_3=\frac{\sqrt{3}}{3}). \quad (3)$$

Then

$$\lambda = \frac{3}{2}\lambda_{100}\left(\alpha_1^2\beta_1^2+\alpha_2^2\beta_2^2+\alpha_3^2\beta_3^2-\frac{1}{3}\right) +3\lambda_{111}(\alpha_1\alpha_2\beta_1\beta_2+\alpha_1\alpha_3\beta_1\beta_3+\alpha_3\alpha_2\beta_3\beta_2). \quad (4)$$

The λ_{111} and λ_{100} are also called the magnetostriction coefficients. These critical parameters of a magnetostrictive material respond for the material's maximum obtainable magnetostriction.

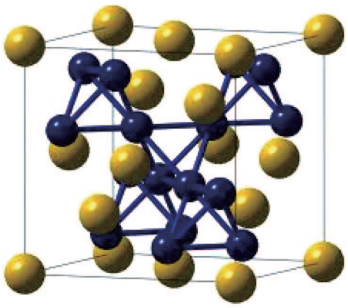


Fig. 1. Crystal structure of *R*Fe$_2$ magnetostrictive compounds. The big balls stand for rare-earth atoms and the small ones for iron atoms.

Since magnetostriction can be defined as the change in dimension of a piece of magnetic material induced by a change in its magnetic state, when a magnetic material is cooled down from its paramagnetic state at high temperature via its T_C to the ferromagnetic/ferromagnetic state at low temperature, due to its spontaneous magnetization and magnetostriction, a structural distortion occurs along its magnetization direction. For instance, paramagnetic *R*Fe$_2$ compound has a cubic MgCu$_2$-type structure; it becomes ferromagnetic/ferrimagnetic tetragonal, rhombohedral, orthorhombic if the magnetization lies along cubic [001], [111], [110], respectively. By using Eq. (4), the magnetization as well as the Weiss equivalent field direction, i.e., the easy magnetization direction (EMD), is the magnetic field direction $[h_1k_1l_1]$, we use $\lambda_{[h_1k_1l_1][h_2k_2l_2]}$ to denote the strain along $[h_2k_2l_2]$, when the magnetization is along $[h_1k_1l_1]$ after magnetostrictive distortion. The interplanar distance of $(h_2k_2l_2)$ becomes our measurement parameter, for the case of the magnetization lying along [001],

$$c=a_0(1+\lambda_{[001][001]})=a_0(1+\lambda_{100}), \quad (5)$$

$$a=a_0(1+\lambda_{[001][100]})=a_0(1-\lambda_{100}/2), \quad (6)$$

$$\frac{\Delta a}{a_0}=\frac{c-a}{a_0}=\frac{3}{2}\lambda_{100}. \quad (7)$$

Here a_0 is the lattice parameter for the cubic structure without magnetostrictive distortion. The distortion ratio $\Delta a/a_0$ is $3\lambda_{100}/2$.

For the case of magnetization lying along [111], the magnetostriction causes a distortion from cubic to rhombohedra structure, and α, β, γ of the cell change from $\pi/2$ to $\psi=\pi/2-\Delta\alpha$, with

$$\Delta\alpha=\lambda_{111}. \quad (8)$$

Proof Figure 2 illustrates the cell after the rhombohedra distortion, where

$$AC^2 = l_+^2 = a_0^2+a_0^2-2a_0^2\cos(\pi/2+\Delta\alpha) = 2a_0^2+2a_0^2\sin\Delta\alpha, \quad (9)$$

$$BD^2 = l_-^2 = a_0^2+a_0^2-2a_0^2\cos(\pi/2-\Delta\alpha) = 2a_0^2-2a_0^2\sin\Delta\alpha. \quad (10)$$

The magnetostriction is on the order of 10^{-3} or less, $\Delta\alpha$ is a small quantity,

$$l_\pm^2 = 2a^2(1\pm\Delta\alpha), \quad (11)$$

$$EO^2 = l_-^2-\left(\frac{l_-}{2}\right)^2=\frac{3l_-^2}{4}=\frac{3}{2}a_0^2(1-\Delta\alpha), \quad (12)$$

$$EO^2 = a_0^2+\left(\frac{l_+}{2}\right)^2-2a_0\frac{l_+}{2}\cos\psi = a_0^2+\frac{a_0^2}{2}(1+\Delta\alpha)-a_0l_+\cos\psi. \quad (13)$$

From Eqs. (12) and (13), one gets

$$a_0l_+\cos\psi=2a_0^2\Delta\alpha, \quad (14)$$

$$CE^2 = AE^2+AC^2-2AC\cdot AE\cdot\cos\psi = a_0^2+l_+^2-2a_0l_+\cos\psi = a_0^2+2a_0^2(1+\Delta\alpha)-4a_0^2\Delta\alpha$$

$$= 3a_0^2\left(1-\frac{2}{3}\Delta\alpha\right). \quad (15)$$

Similarly,

$$\begin{aligned} AG^2 &= a_0^2 + l_+^2 + 2a_0 l_+ \cos\psi \\ &= a_0^2 + 2a_0^2(1+\Delta\alpha) + 4a_0^2\Delta\alpha = 3a_0^2(1+2\Delta\alpha), \end{aligned} \quad (16)$$

$$\begin{aligned} AG - CE &= \sqrt{3}a_0(1+\Delta\alpha) - \sqrt{3}a_0\left(1-\frac{\Delta\alpha}{3}\right) \\ &= \frac{4}{3}\sqrt{3}a_0\Delta\alpha. \end{aligned} \quad (17)$$

From the aspect of magnetostriction and Eq. (4), using $\alpha_1 = \alpha_2 = \alpha_3 = 1/\sqrt{3}$ and $\beta_1 = \beta_2 = \beta_3 = 1/\sqrt{3}$, one has

$$\lambda_{[111][111]} = \frac{AG - \sqrt{3}a_0}{\sqrt{3}a_0} = \lambda_{111}. \quad (18)$$

When $\alpha_1 = \alpha_2 = \alpha_3 = 1/\sqrt{3}$ and $\beta_1 = \beta_2 = -\beta_3 = 1/\sqrt{3}$, one has

$$\lambda_{[111][11\bar{1}]} = \frac{CE - \sqrt{3}a_0}{\sqrt{3}a_0} = \frac{1}{3}\lambda_{111}. \quad (19)$$

Hence

$$AG - CE = \frac{4}{3}\sqrt{3}a_0\lambda_{111}. \quad (20)$$

Comparing Eq. (17) with Eq. (20), equation (8) is seen to be distinct.

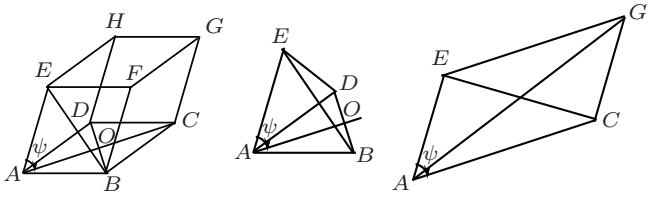


Fig. 2. RFe$_2$ crystal cell after rhombohedral magnetostrictive distortion.

2.2. Measurement technology for magnetostriction

Magnetostriction is a micro-strain, which can be measured by using a Michelson interferometer, an optical lever measurement system, a strain gauge, a dilatometer, or the capacitance techniques (in which the strained material displaces a capacitor plate). A strain gauge made from an electrical resistance string is the most commonly used element for magnetostriction measurement. It is typically mounted in a plane of the sample and has the same length change as the sample. Magnetostriction in proportion to the resistance of the strain gauge is measured by a strain gauge indicator based on the Wheatstone bridge.

The magnetostriction coefficients λ_{111} and λ_{100} may be obtained by measuring either a single crystal or polycrystalline sample. For the former, the measurement may be directly performed along the [111] or [100] direction of a single crystal under relatively high magnetic fields; while for the latter, the measurement is implemented by using an X-ray diffraction technique to detect the structural distortion of the magnetostrictive phase without any magnetic fields. Although the direct measurement may reach a high precision, even better than 1 ppm (1 ppm = 10^{-6}), it is not easy to obtain a large single crystal for the magnetostriction measurement, and errors also arise from the initial magnetization state. The indirect polycrystalline method is simple and sample-insensitive, the precision is determined by the measurement of crystallographic parameters. For θ–2θ step scanning X-ray diffraction (XRD) technology, only magnetostriction larger than 1000 ppm may be measured. But precision of 200–500 ppm may be reached if the synchrotron XRD or neutron diffraction is applied to measure the lattice parameters.[13] Magnetostriction in RFe$_2$ compounds is highly anisotropic, $\lambda_{111} \gg \lambda_{100}$, when the magnetic moment lies along [100], and the structural distortion resulting from the magnetostriction is so fine that it cannot be identified by a crystallographic method; however it can be determined by the XRD technique when the EMD lies along [111]. According to the relationship between structural distortion and magnetostriction, the structure of RFe$_2$ becomes rhombohedral, meaning many cubic reflections double-split or multi-split.[14] The splitting distance is determined by Eq. (4) with $\alpha_1 = \alpha_2 = \alpha_3 = 1/\sqrt{3}$.

(A) For (110)-type reflections,

$$\begin{aligned} d_{110} &= d^0_{110}(1+\lambda_{[111][110]}) = d^0_{110}\left(1+\frac{1}{2}\lambda_{100}+\frac{1}{2}\lambda_{111}\right), \\ &\quad (\beta_1 = \beta_2 = \sqrt{2}/2, \quad \beta_3 = 0), \end{aligned} \quad (21)$$

$$\begin{aligned} d_{1\bar{1}0} &= d^0_{110}(1+\lambda_{[111][1\bar{1}0]}) = d^0_{110}\left(1+\frac{1}{2}\lambda_{100}-\frac{1}{2}\lambda_{111}\right), \\ &\quad (\beta_1 = \sqrt{2}/2, \quad \beta_2 = -\sqrt{2}/2, \quad \beta_3 = 0). \end{aligned} \quad (22)$$

So, the (110)-type reflections double-split, combining different magnetization directions [111], [1$\bar{1}$1], [11$\bar{1}$], [1$\bar{1}\bar{1}$] with different measurement directions [110], [1$\bar{1}$0], [101], [10$\bar{1}$], [011], [01$\bar{1}$]; the theoretical strong ratio for the split reflection is 1:1, and

$$\lambda_{111} = \frac{d_{110} - d_{1\bar{1}0}}{d^0_{110}}. \quad (23)$$

After the magnetostrictive distortion, d^0_{110} is not obtained directly; however, it can be taken as the average value of the interplanar distance of (110) and (1$\bar{1}$0) because of the negligibility of λ_{100} in RFe$_2$, hence

$$\lambda_{111} = 2\frac{d_{110} - d_{1\bar{1}0}}{d_{110} + d_{1\bar{1}0}}. \quad (24)$$

(B) For (111)-type reflections, it is also easy to obtain that the reflections double-split with a strong ratio of 1:3 and

$$\lambda_{111} = \frac{3}{4}\frac{d_{111} - d_{11\bar{1}}}{d^0_{111}}. \quad (25)$$

(C) For (100)-type reflections, they do not split when the magnetization lies along ⟨111⟩. To study the magnetostriction of $R\mathrm{Fe}_2$ compounds, the (440) reflection and equation (24) are always used to determine the magnetostriction coefficient λ_{111}.

3. Progress with rare-earth-Fe_2 magnetostrictive compounds and alloys since the 1990s

3.1. Further studies on Terfenol-D

Terfenol-D is a milestone in the development of magnetostrictive materials. It has a single-crystal magnetostriction as large as 1600 ppm under a relatively small magnetic field without any stress bias at RT. After it was discovered, further decreases in anisotropy were expected to be found in multicomponent pseudobinary systems such as $\mathrm{Tb}_x\mathrm{Dy}_y\mathrm{Ho}_z\mathrm{Fe}_2$. $\mathrm{Tb}_{0.20}\mathrm{Dy}_{0.22}\mathrm{Ho}_{0.58}\mathrm{Fe}_2$ was found to have small anisotropy constants K_1 and K_2, but much smaller saturation magnetostriction λ_s than Terfenol-D.[15] Later, a more systematic investigation was made by Restorff *et al.* They did not focus only on anisotropy, but also considered magnetic field, temperature, and stress dependencies of the magnetostriction and hysteresis loss of different $\mathrm{Tb}_x\mathrm{Dy}_y\mathrm{Ho}_z\mathrm{Fe}_2$ alloys. Many Ho-containing alloys have extreme magnetostrictive properties, e.g., very low hysteresis loss (area of the hysteresis loop) with only slightly lower magnetostriction.[16] Much research work has been done on the substitution of Mg, Al, Ga, Si and almost all the 3d transition metals for Fe in Terfenol-D, in an effort to further improve its magnetic and magnetostrictive properties.[17–32] However, few of the substitutions essentially improve the desired properties; conversely, most of them decrease the magnetostriction of Terfenol-D at RT. Indeed, the superexcellent magnetostriction properties of the Terfenol-D are difficult to surpass, but a further reason might be that, in Terfenol-D, the anisotropy is minimized by modulating the Tb/Dy ratio, and a substitution for Fe induces an increase of anisotropy. A typical case is the substitution of Co for Fe,[19] it was found that the substitution of Co for Fe enhances the spin reorientation temperature T_{SR} of Terfenol-D. The low anisotropy of Terfenol-D can be ascribed to its T_{SR} near RT. At T_{SR}, the magnetocrystalline anisotropy should be almost zero, accompanying the change of the easy magnetization direction. The change of T_{SR} results in the deviation of the anisotropy from its minimum value. Considering the anisotropy nature of Tb^{3+} (decreasing T_{SR}) and Dy^{3+} ions (increasing T_{SR}),[1] it was deemed that a new improved magnetostrictive material containing Co could be formed, which should also have optimum performance at RT. In fact, the work of Liu *et al.*,[33] Ma *et al.*,[34–38] and Jiang *et al.*[39] have proved this viewpoint. In the Co-substituted Terfenol-D system, the composition for the compensation of the anisotropy (anisotropy minimized) shifts to the Tb-rich side where it has a larger magnetostriction coefficient λ_{111} than Terfenol-D. Moreover, the substitution of Co for Fe changes the fill of the 3d band, leading the magnetostriction coefficient λ_{100} to increase from almost zero for the un-substituted compound to 700–1000 ppm for about 20% Co substitution (Fig. 3).[33] The exceptionally improved magnetostrictive properties may be ascribed to the almost unchanged magnetic moment and increased T_{C} when the Co content is between 15% and 30% among transition metals, as well as to the anisotropy compensation achieved in the compound.[33–39]

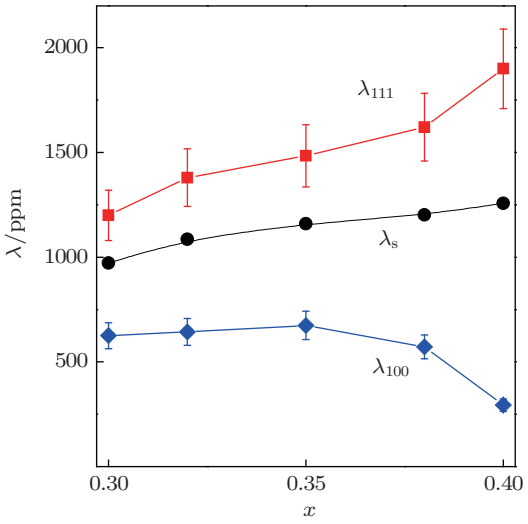


Fig. 3. Composition dependence of saturation magnetostriction λ_s and spontaneous magnetostriction λ_{111} and λ_{100} for $\mathrm{Tb}_x\mathrm{Dy}_{1-x}(\mathrm{Fe}_{0.8}\mathrm{Co}_{0.2})_2$ compounds.[33]

Due to the highly anisotropic magnetostriction of $R\mathrm{Fe}_2$ compounds, single crystals or aligned polycrystalline samples possess much better magnetostrictive properties than polycrystals with randomly oriented grains. It was reported that it is difficult to grow the [111] oriented crystal, while [112] twinned crystals could be easily obtained due to the preferred growth along the [112] direction.[40] In 1988, a magnetostriction jump of ∼ 800 ppm was observed in twinned [112] Terfenol-D rod at 250 Oe under a pre-stress of 7.6 MPa. A similar jump was found in the [110] oriented Terfenol-D crystals grown at a high velocity, however, no such jump appears in the [110] oriented crystals grown at a low velocity. Single and two {111}-twin system growth mechanisms were proposed to interpret the divergence.[41] In 1995, [111] oriented Terfenol-D was grown by Wu *et al.* using the Czochralski method with an induction heating magnetic levitation cold crucible.[42] The magnetostriction was measured along [111], [11$\bar{2}$], and [1$\bar{1}$0] directions with an applied magnetic field of 20 kOe rotating in the (11$\bar{2}$) and (1$\bar{1}$0) planes.[43] The measured magnetostriction along the [111] direction is 1640 ppm, which is quite consistent with the value calculated by the XRD crystallographic method performed on polycrystalline Terfenol-D. It increases with increasing compressive stress applied along the rod axis, and reaches 2375 ppm under a stress of 24 MPa.

Thereafter, Du *et al.*[44] investigated the twin-free single crystals $Tb_xDy_{1-x}Fe_2$ with the addition of aluminum and manganese. It was found that the measured magnetostriction along [111] of $Tb_{0.5}Dy_{0.5}(Fe_{0.9}Mn_{0.1})_2$ was about 200 ppm when no compressive pre-stress was applied. A large increase of about 2000 ppm, shown in Fig. 4, was detected when the pre-stress was increased to 21 MPa under a saturation field of 900 Oe. A distinct jump was found in the field dependence of magnetostriction under the pre-stress of 21 MPa. It is believed that these observations foreshadow more materials with excellent magnetostrictive properties, quite possibly surpassing those reported in twinned Terfenol-D.[9] The average static $d_{33} = \lambda_{\parallel}/H$ (where $\lambda_{\parallel}$ is the parallel magnetostriction) during the whole jumping process of the magnetic field from 600 Oe to 800 Oe is about 4.8 ppm/Oe. Even a maximum of 6.5 ppm/Oe has been observed.[44]

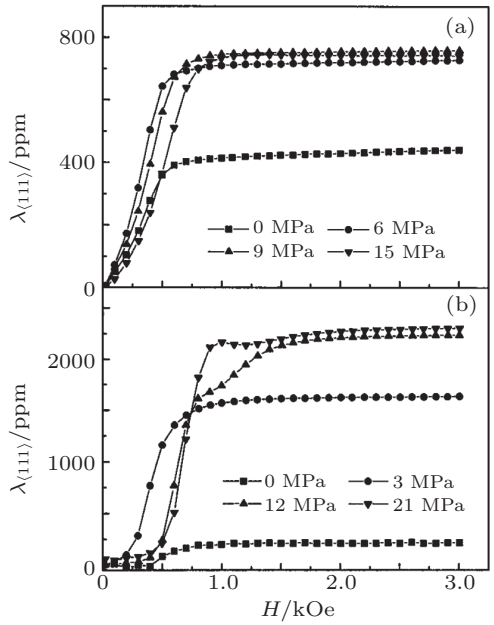


Fig. 4. Magnetostriction under different compressive stresses as a function of the applied field for (a) $Tb_{0.27}Dy_{0.73}(Fe_{0.85}Al_{0.15})_2$ and (b) $Tb_{0.5}Dy_{0.5}(Fe_{0.9}Mn_{0.1})_2$.[44]

Much attention has also been paid to the effects of small atoms, such as C,[45] Be,[46] and B,[47] as interstitial/substitutional atoms on the structural and magnetic characteristics of the cubic Laves phases. The carbon modified Terfenol-D $Tb_{0.3}Dy_{0.7}Fe_2C_x$ distorts to a tetragonal structure subjected to the asynchronous increase of lattice parameters a and c. Carbon atoms occupy the interstitial sites, but T_C hardly changes, which is abnormal, as other interstitial atoms lead to increasing T_C. Magnetostriction at 20 kOe hardly changes when $x \leq 0.1$, but decreases at low magnetic field. It is reasonable to think that interstitial C atoms hamper the motion of domain walls and the rotation of the moment without changing the structural and intrinsic magnetic properties.[45] The lattice parameter for Be-modified compounds $Tb_{0.3}Dy_{0.7}(Fe_{1-x}Be_x)_2$ decreases with increasing Be content (the reverse of the behavior of carbon-modified Terfenol-D), indicating that the Be atoms occupy the substitutional sites. Saturation magnetization M_s and T_C decrease with increasing Be content, arising from the dilution effect and the decrement in Fe–Fe and R–Fe exchange interactions due to the substitutional diamagnetic Be. A maximum magnetostriction of 1235 ppm under 20 kOe was obtained in the $x = 0.1$ alloy. This value is higher than that of the base alloy. The low-field magnetostriction was found to be greatly enhanced due to the addition of Be.[46] The boron-doped $Tb_{0.27}Dy_{0.73}Fe_2B_x$ alloy was found to effectively restrain the emergence of the RFe_3 iron-rich (1:3) phase; magnetostriction increases with the doping B content when $x < 0.2$. The authors believed that the peritectic point shifts slightly, and therefore, B doped Terfenol-D forms directly, so it is easy to form single phase Terfenol-D materials. The lattice parameter and B-occupied sites were not identified in that work.[47] Thereafter, B was introduced to $Tb_{0.7}Pr_{0.3}Fe_2$ and $Dy_{0.7}Pr_{0.3}Fe_2$, both containing large amounts of 1:3 impurity phase. It was confirmed that B inhibits the emergence of the 1:3 phase and therefore improves the magnetostrictive properties.[48,49] In $Tb_{0.7}Pr_{0.3}(Fe_{1-x}B_x)_2$, the lattice parameter increases with increasing boron concentration up to $x = 0.10$ and decreases with a further increase of x, showing that boron preferentially occupies the interstitial sites when its concentration does not reach the solubility limit $x = 0.10$ (about 6.67 at.%). Above this limit, boron starts to occupy the Fe substitutional sites.[48] However, in $Dy_{0.7}Pr_{0.3}(Fe_{1-x}B_x)_2$, the lattice parameter decreases with increasing B concentration from the beginning of doping. Boron atoms directly occupy the Fe substitutional sites.[49] That B atoms may occupy the interstitial sites in $Tb_{0.7}Pr_{0.3}(Fe_{1-x}B_x)_2$, which may be related to the large magnetostrictive distortion along its [111] EMD. Lattice parameter a depends on small atoms for $Tb_{0.7}Pr_{0.3}(Fe_{1-x}B_x)_2$, $Tb_{0.7}Pr_{0.3}(Fe_{1-x}B_x)_2$, and $Tb_{0.3}Dy_{0.7}(Fe_{1-x}Be_x)_2$, as represented in Fig. 5. The investigation of small-atom modified magnetostrictive compounds indicates that the optimal addition of small atom is $\sim$ 3–6 at.% for either interstitial or substitutional occupation.

Properties other than large magnetostriction and small anisotropy, such as small hysteresis, large impedance or resistance, good ductility, and so forth, are also of importance for practical applications of magnetostrictive materials. To determine the hysteresis, the piezomagnetic coefficient d_{33} is measured with or without stress bias in a sinusoidal magnetic drive field H_3, usually of 450 Oe (amplitude), with a fixed frequency, together with various magnetic bias fields H_{bias}. The hysteresis width W_h is defined as the average width of the $\lambda_{\parallel}$–H (sum magnetic field) curve at H_{bias}, where d_{33} has a maximum.[50,51] It has been found that the addition of Ho reduces the W_h of

polycrystalline and [112] oriented Terfenol-D.[50,51] The W_h of [110] oriented $Tb_{0.29}Dy_{0.48}Ho_{0.23}Fe_2$ single crystal decreases linearly with increasing temperature from −60 °C to 80 °C.[52] The hysteresis of a [110] oriented Tb–Dy–Fe crystal nearly disappears under compressive pre-stress of about 120 MPa.[53] Prajapati *et al.* found that the substitution of Al for 10% of the Fe in Terfenol-D produces a material with potential benefits for use in actuators: higher electrical resistivity thereby lowers eddy current losses and improved ductility increases the mechanical strength, while maintaining the large magnetostriction of 1200 ppm at approximately 1.5 kOe with a magnetomechanical coupling coefficient K_{33} of ∼ 62% and a large d_{33} of ∼ 1 ppm/Oe.[54] A drastic increase of electrical resistivity and a visually improved corrosion resistance (in a 3.5 wt.% NaCl aqueous solution) were observed by Xu *et al.* upon substituting a small amount of Si for Fe in Terfenol-D.[55,56]

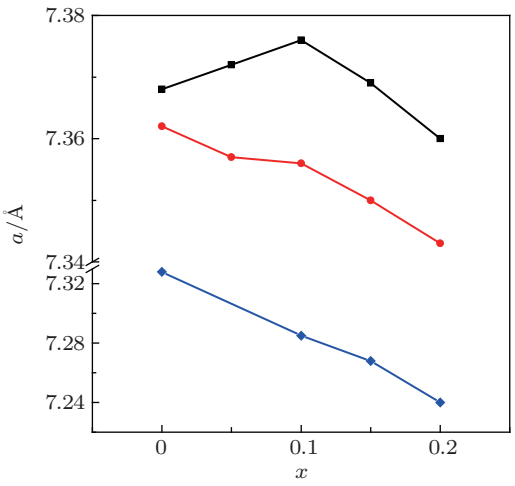


Fig. 5. Lattice parameter for $Tb_{0.7}Pr_{0.3}(Fe_{1-x}B_x)_2$ (square),[48] $Dy_{0.7}Pr_{0.3}$ $(Fe_{1-x}B_x)_2$ (circle),[49] and $Tb_{0.3}Dy_{0.7}$ $(Fe_{1-x}Be_x)_2$ (diamond).[46]

3.2. Studies of light rare-earth magnetostrictive materials

3.2.1. Magnetostrictive compounds containing light rare-earth Ce

$CeFe_2$ is a very special Laves compound. Its T_C is 235 K, much lower than that of other RFe_2, which is typically 500–700 K. Its lattice parameter is 7.303 Å, an exceptional case of lanthanum contraction of RFe_2.[57] The single-ion approach predicts that the magnetostriction of $CeFe_2$ at 0 K is 6000 ppm, the largest value of the series compounds;[1] however, the measured magnetostriction is small. It is believed the non-3^+ valence distribution is the most likely reason. Tang *et al.* systematically investigated the structural, magnetic, and magnetostrictive properties of pseudobinary (Ce, R)Fe_2 compounds.[58–61] The Ce content dependencies of the lattice parameter, T_C, and the hyperfine field of Fe of the compounds strongly suggest that the degree of delocalization of Ce 4f electrons varies with both the magnitude of the substitution and the choice of rare-earth element. The degree of delocalization is enhanced when R is the light rare-earth Pr,[58] and is degraded when R is the heavy rare-earth Tb or Dy,[59,60] while it changes little when R is Nd.[61] A metamagnetic phase transition can be observed in both $Ce_xTb_{1-x}Fe_2$ and $Ce_xDy_{1-x}Fe_2$, when the Ce concentration x is about 0.5. The critical phase field increases with the Ce concentration, embedding the abundant special physical properties of $CeFe_2$; the itinerant-electron model has been applied to analyze the tendency toward change of the critical field with x.[60] The magnetostriction of these compounds was measured only at RT, the evidence of $CeFe_2$ with a very large magnetostriction has not been found.

3.2.2. Magnetostrictive compounds containing light rare-earth Pr

Based on the single-ion approach, the rare-earth sublattice contributes to magnetostriction λ_{111}, the intrinsic λ_{111} ($T = 0$ K) of RFe_2 can be given by calculation. Relative to λ_{111} of 4400 ppm for $TbFe_2$, the calculated λ_{111} at 0 K for $PrFe_2$ is 5600 ppm.[1] $PrFe_2$ cannot be synthesized at ambient pressure because of the large radius of Pr^{3+} against the size match of the Laves phase.[62] Experimental magnetostriction $\lambda_{\parallel} - \lambda_{\perp}$ at RT was measured to be 1030 ppm by Zhao *et al.* using the sample containing impurities synthesized at high pressure.[63] This value is not very large, but that is due to the influence of impurities and the state of the particular sample (not ingot). Many other experiments suggested that λ_{111} of $PrFe_2$ at RT should be no lower than 2000 ppm, much larger than the 1260 ppm measured for $DyFe_2$. Thus, much attention has been paid to the magnetostrictive compounds containing Pr. Also because of the large radius of Pr^{3+}, in (R, Pr)Fe_2 compounds, when Pr is over 20% among the rare-earths, a single Laves phase cannot be reached. Therefore, Wu *et al.* did many studies on the magnetostrictive compounds containing 10% Pr among the rare-earths: typical rare-earth compositions, such as $Dy_{0.60}Tb_{0.30}Pr_{0.1}$ and $Dy_{0.65}Tb_{0.25}Pr_{0.1}$, with Fe substituted by Mn,[64] Al,[65] Ga,[66] and Cr.[66] It was found that either the substitution of 5% Al or 2% Cr among transition metals for Fe in $Dy_{0.65}Tb_{0.25}Pr_{0.1}Fe_{1.85}$ or 5% Mn substitution for Fe in $Dy_{0.60}Tb_{0.30}Pr_{0.1}Fe_{1.85}$ leads to a slight increase of $\lambda_{\parallel} - \lambda_{\perp}$ at low field of less than 2–4 kOe.[64–66] The reason, confirmed by micro-analysis, is that the substitutions help the formation of the Laves phase and inhibit the appearance of the 1:3 impurity phase. But λ_{111} decreases with the substitutions. These results are consistent with the studies of Fe-site substitution in Terfenol-D. The reason remains unknown, since the studies of the anisotropy of these compounds are insufficient.

Cobalt or nickel was substituted for Fe to enhance the Pr content in (R, Pr)Fe_2 Laves phase, due to the fact that it is easy to synthesize both $PrNi_2$ and $PrCo_2$ cubic Laves phases at ambient pressure. It was found that the 1:2 phase exists in the entire composition range of $Tb_{1-x}Pr_x(Fe_{0.4}Co_{0.6})_2$ alloys. The 1:3 impurity phase appears and coexists with the

1:2 Laves phase when $x \geq 0.2$. Figure 6 shows the relative amount of (Tb, Pr)(Fe, Co)$_2$ phase decreasing with increasing Pr content but exhibiting a peak near $x = 0.5$, and increasing with increasing x in the range $0.7 < x < 1.0$. The anomaly at 0.5 exists because another Tb–Pr δ impurity phase forms,[67] which leads the Pr content in the Laves phase to decrease, benefiting the formation of the Laves phase, and thus the ratio of 1:2 phase to 1:3 phase increases.[68] The matrix of the homogenized $Dy_{1-x}Pr_xFe_2$ alloys is the 1:2 Laves phase; the 1:3 phase appears and increases with increasing Pr content and becomes the main phase when $x = 0.4$. When $x = 0.5$, the main phase is (Dy, Pr)$_2$Fe$_{17}$ (2:17) with Th$_2$Zn$_{17}$-type structure and the three other phases which are present in small amounts are 1:2, 1:3, and a rare-earth rich phase.[69] When Co is substituted for Fe in $Dy_{0.6}Pr_{0.4}Fe_2$, the amount of the 1:3 phase decreases with increasing Co content x until $x = 0.6$; then the 1:2 phase becomes the main phase.[69] As the main phase of the $Tb_{0.6}Pr_{0.4}(Fe_{0.4}Co_{0.6})_2$ alloy is the 1:3 phase,[68] it is clear that the element Dy is more conducive to the formation of the cubic Laves phase than element Tb when the Pr content is high. And the main phase of the $Dy_{0.6}Pr_{0.4}(Fe_{0.4}Ni_{0.6})_2$ alloy remains the 1:3 phase after partial Ni substitution for Fe.[69] It is evident that the element Co is more beneficial for the formation of the 1:2 Laves phase than the element Ni. The stabilizing effect of Co on the 1:2 Laves phase with high Pr content was further demonstrated by Liu *et al.* Figure 7 shows that a single Laves phase forms in $Tb_{0.2}Pr_{0.8}(Fe_{1-x}Co_x)_2$ when Co exceeds 65% of the transition metal.[70] In $Dy_{0.6}Pr_{0.4}(Fe_{1-x}Co_x)$ and $(Tb_{0.7}Dy_{0.3})_{0.7}Pr_{0.3}(Fe_{1-x}Co_x)_{1.85}$, the R-sublattice is invariant, and T_C depends on the transition metal sublattice. The composition dependencies of T_C of the Laves phase in both alloys have the same trend as the Slater–Pauling curve for the moment of Fe–Co alloys, displaying a maximum at about $x = 0.3$. The magnetization of the $(Tb_{0.7}Dy_{0.3})_{0.7}Pr_{0.3}(Fe_{1-x}Co_x)_{1.85}$ alloy possesses a minimum value at $x = 0.3$, which originates from the antiparallel alignment of the moment of total rare-earth $m_{Dy+Tb-Pr}$ and total transition-metal moment m_{Fe+Co}, where the moment of $Fe_{1-x}Co_x$ has a maximum value.[69,71] Because of the formation of the Tb–Pr δ phase, the Pr content in the Laves phase decreases, λ_{111} for $Tb_{1-x}Pr_x(Fe_{0.4}Co_{0.6})_2$ obtains a minimum value at $x = 0.5$. While $\lambda_{\parallel} - \lambda_{\perp}$ has a complex dependence as in Fig. 8.[68] However, it agrees well with the relative amount of the 1:2 magnetostrictive phase (Fig. 6). When $x = 0.5$, λ_{111} has a minimum value, the increasing trend caused by the increasing amount of the Laves phase overcomes the decreasing trend caused by the decrease of λ_{111}. The composition for the compensation of anisotropy was determined to be $x = 0.8$.[68] This is reasonable in view of the following facts. (i) The anisotropy of Tb^{3+} is much larger than that of Pr^{3+}. (ii) The EMD of $PrFe_2$ and $PrCo_2$ lies along [100] at low temperature, while that of $PrFe_2$ lies along [111] and $PrCo_2$ is paramagnetic at RT. It is possible that the EMD of $Pr(Fe_{0.4}Co_{0.6})_2$ lies along [100], while that of $Tb(Fe_{0.4}Co_{0.6})_2$ lies along [111] due to the [111] EMD for both $TbFe_2$ and $TbCo_2$.[57] Magnetostriction of $Dy_{0.6}Pr_{0.4}Fe_2$ decreases with Co and Ni substitutions for Fe, both substitutions lead to a negative magnetostriction when the substitution amount is larger than 40% Fe, and Ni leads to a more drastic reduction than Co.[69] The high Dy content together with a high Co content render a composition approaching $DyCo_2$, which has a large negative magnetostriction λ_{100},[72] yielding the negative magnetostriction. In all the studied compositions $(Tb_{0.7}Dy_{0.3})_{0.7}Pr_{0.3}(Fe_{1-x}Co_x)_{1.85}$, $\lambda_{\parallel} - \lambda_{\perp}$ deceases with increasing Co content x, but no negative magnetostriction was observed in this system.[71]

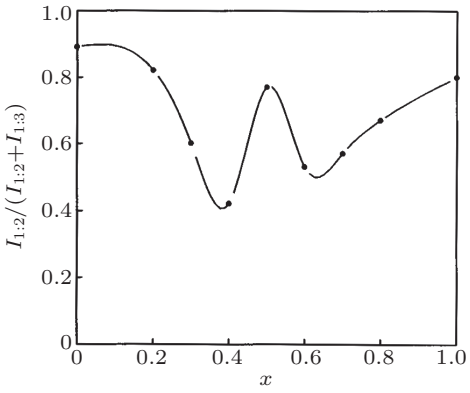


Fig. 6. Pr composition dependence of the proportion of (Tb, Pr) (Fe, Co)$_2$ phase in the $Tb_{1-x}Pr_x(Fe_{0.4}Co_{0.6})_{1.9}$ alloys.[68]

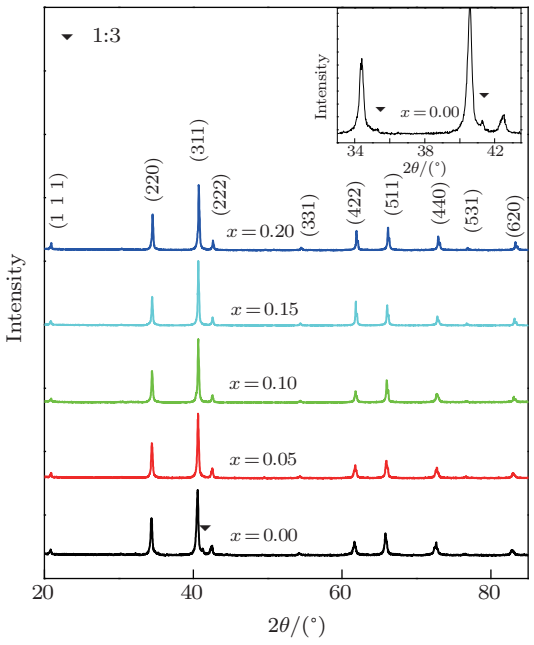


Fig. 7. X-ray diffraction patterns of $Tb_{0.2}Pr_{0.8}$ $(Fe_{0.4-x}Co_{0.6+x})_{1.93}$ alloys ((h,k,l) of the Laves phase is indexed). For clarity, the insert shows the impurity peaks when $x = 0$.[70]

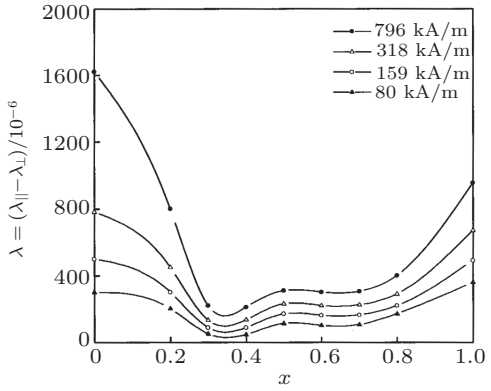


Fig. 8. Pr composition dependence of magnetostriction $\lambda_{\parallel} - \lambda_{\perp}$ at room temperature for annealed polycrystalline $Tb_{1-x}Pr_x(Fe_{0.4}Co_{0.6})_{1.9}$ alloys.[68]

It has been reported that the introduction of a small amount of boron can effectively inhibit the presence of the 1:3 impurity phase in $Tb_{0.27}Dy_{0.73}Fe_2$,[47] $Tb_{0.7}Pr_{0.3}Fe_2$,[48] and $Dy_{0.7}Pr_{0.3}Fe_2$.[49] So it is interesting to know the upper limit of Pr content to form single Laves phase in (*R*, Pr)(Fe, B)$_2$/(R, Pr)Fe_2B_δ alloys, where the different formats depend on the B substitutional/interstitial sites in the alloys. In $Tb_xDy_{0.7-x}Pr_{0.3}(Fe_{0.9}B_{0.1})_2$, at both Tb-rich and Dy-rich ends, single Laves phases form, but when x is about 0.4, very small amounts of impurity phases, such as rare-earth, 2:17 phase, coexist.[73] In $Tb_{1-x}Pr_xFe_{1.93}B_{0.15}$[74] and $Tb_{0.2}Dy_{0.8-x}Pr_x(Fe_{0.9}B_{0.1})_2$,[75] the single Laves phase forms up to $x = 0.4$. A detailed investigation of the latter system shows that the saturation magnetization M_s of the alloys linearly decreases with increasing Pr content when $x \leq 0.34$, and deviates from the linear rule when $x \geq 0.37$, suggesting that 0.34 is the upper limit of the Pr content for the formation of the single Laves phase in the system.[76] In $Dy_{1-x}Pr_x(Fe_{0.9}B_{0.1})_2$,[77] the inhibitory action of B on the presence of the 1:3 phase is weaker than that in the $Tb_{1-x}Pr_xFe_{1.93}B_{0.15}$ system; when $x = 0.4$, a large amount of 1:3 impurity phase appears. Since in these two systems, B atoms occupy different sites, it seems that the interstitial boron atoms are more beneficial to the formation of the Laves phase than the substitutional ones. In $Tb_{0.1}Ho_{1-x}Pr_x(Fe_{0.9}B_{0.1})_2$, the single phase also forms up to $x = 0.3$.[78] Liu *et al.* introduced a small amount of B to $Tb_{0.2}Pr_{0.8}(Fe_{0.4}Co_{0.6})_{1.93-x}B_x$, finding that a single Laves phase can form when $0.05 \leq x \leq 0.35$. Composition dependencies of T_C and the lattice parameter show that B is at the interstitial sites.[79] A further investigation shows that the $Tb_{1-x}Pr_x(Fe_{0.4}Co_{0.6})B_{0.1}$ alloys in the whole concentration range of $0 \leq x \leq 1$ are 1:2 Laves single-phase.[80] Similarly, single-phase $Dy_{1-x}Pr_x(Fe_{0.35}Co_{0.55}B_{0.1})_2$[81] and $Nd_{1-x}Pr_x(Fe_{0.35}Co_{0.55}B_{0.1})_2$[82] Laves compounds were synthesized in the whole range of $0 \leq x \leq 1$.

The molecular radius of $PrFe_2$ is 7.467 Å, much larger than 7.347 Å for $TbFe_2$ and 7.325 Å for $DyFe_2$, the T_C of $PrFe_2$ is 543 K, much lower than 704 K for $TbFe_2$ and 638 K for $DyFe_2$.[1,83] In all (*R*, Pr)Fe_2, (*R*, Pr)Fe_2B_δ, (*R*, Pr)(Fe, B)$_2$, (*R*, Pr)(Fe, Co, B)$_2$ alloys, when *R* is Tb, Dy, Ho, Nd, or their composite (excluding Ce), if the single Laves phase was obtained, both T_C and the lattice parameter of the phase obey the linear Vegard's law. $PrFe_2$ is ferromagnetic, the Pr moment aligns parallel to the Fe moment, while heavy rare-earth compounds RFe_2, such as $TbFe_2$, $DyFe_2$, and $HoFe_2$, are ferrimagnetic, the *R* moment aligns antiparallel with the Fe moment, and the heavy rare-earth moment is larger than the Fe moment. Thus, the Pr substitution always leads to a decrease of magnetization. Figure 9 displays the compensation of magnetization in $Tb_{1-x}Pr_x(Fe_{0.4}Co_{0.6})_{1.9}B_{0.1}$[80] at both 5 K and RT, which was also observed in $Dy_{1-x}Pr_x(Fe_{0.35}Co_{0.55}B_{0.1})_2$.[81]

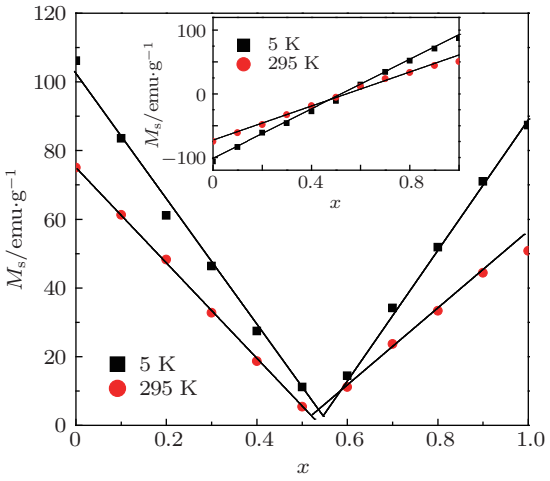


Fig. 9. Composition dependence of the saturation magnetization M_s of $Tb_{1-x}Pr_x(Fe_{0.4}Co_{0.6})_{1.9}B_{0.1}$ compounds at 5 K and 295 K. Inset: the magnetic moment σ_s per formula unit of $Tb_{1-x}Pr_x(Fe_{0.4}Co_{0.6})_{1.9}B_{0.1}$.[80]

A large magnetostriction is essential for a practical magnetostrictive material. Thus, the magnetostriction coefficient λ_{111} is of utmost importance, and it implies the magnetostrictive potential of the compound because $\lambda_{111} \gg \lambda_{100}$ in RFe_2. Limited by the accuracy of the XRD structural analysis, only a λ_{111} larger than 1000 ppm can be determined by this method, usually, by analyzing the (440) line of the compound and using Eq. (4). In $Tb_{1-x}Pr_xFe_{1.93}B_{0.15}$, λ_{111} is almost invariant, or more specifically, it decreases slightly with increasing Pr content. This tendency is consistent with the previous results of Clark *et al.*[84] According to the single-ion approach, the magnetostriction λ_{111} is determined by the anisotropy of the rare-earth element. Thus, it can be concluded that the λ_{111} of $PrFe_2$ is slightly smaller but still comparable with that (2460 ppm) of $TbFe_2$. In $Tb_{0.2}Dy_{0.8-x}Pr_x(Fe_{0.9}B_{0.1})_{1.93}$, λ_{111} monotonically increases with x increasing, thus $PrFe_2$ should have a larger λ_{111} than $DyFe_2$.[75] The λ_{111} of $DyFe_2$ is 1260 ppm as extrapolated by Clark *et al.* from $Tb_{1-x}Dy_xFe_2$ compounds.[1,85] In $Dy_{0.7-x}Tb_xPr_{0.3}(Fe_{0.9}B_{0.1})_{1.93}$,[73] the λ_{111} of the alloy with $x = 0.25$ is 1850 ppm, larger than 1600 ppm for

$Tb_{0.27}Dy_{0.73}Fe_2$. It was consistently found that the λ_{111} of $PrFe_2$ is larger than that of $DyFe_2$.

Since the anisotropy constants K_1 of $PrFe_2$ and $DyFe_2$ have the same sign, $Dy_{1-x}Pr_xFe_2$ used to be considered as a non-compensating system according to Clark's lowest order anisotropy theory. However, the EMD of $DyFe_2$ lies along [100] while that of $PrFe_2$ lies along [111] at RT. Ren *et al.* proposed that in this system, and of course, in the compounds it represents, the effects of the anisotropy constant K_2 must be taken into account. They phenomenologically demonstrated that the composition for compensation of the anisotropy in $Dy_{1-x}Pr_xFe_2$ systems is obtainable based on the single-ion approach.[75]

The experimental evidences for this include the followings.

(i) Tang *et al.* calculated the K_1 of $Dy_{0.9-x}Pr_xTb_{0.1}Fe_2$ by using the approach-to-saturation law of the polycrystalline samples, finding that K_1 decreases with increasing Pr content. The minimum value of K_1 was not obtained, suggesting that the complete compensation of anisotropy was not achieved, since a single phase compound with enough Pr content was not obtained.[86]

(ii) The (440) line of the Laves phase in Fig. 10 is a single peak for the $Tb_{0.2}Dy_{0.8-x}Pr_x(Fe_{0.9}B_{0.1})_{1.93}$ alloys with $0 \leq x \leq 0.3$. This means that the EMD lies along the [100] axis. Only a tiny distortion of the crystal structure originating from magnetostriction is realized ($\lambda_{100} \approx 0$) and XRD peak splitting is not observed. Nevertheless, the double split (440) lines of the Laves phase are clearly observed in the alloys with $0.4 \leq x \leq 0.7$. This indicates the EMD lies along the [111] axis and a large rhombohedral distortion occurs due to magnetostriction, contributing to a large splitting of the (440) XRD line. In the $Tb_{0.2}Dy_{0.8-x}Pr_x(Fe_{0.9}B_{0.1})_{1.93}$ alloys, the Tb content is invariant. The change of the EMD is determined by the content change between Pr and Dy. This indicates that the anisotropy of $PrFe_2$ and $DyFe_2$ can compensate with each other.[75]

(iii) The T_{SR} for the $Tb_{0.2}Dy_{0.8-x}Pr_x(Fe_{0.9}B_{0.1})_{1.93}$ alloys decreases from 365 K across RT to 240 K as x is increased from 0.18 to 0.40. The EMD of the Dy-rich alloys with $T_{SR} >$ RT prefers to lie along the [100] axis at RT, whereas that of the Dy-poor alloys with $T_{SR} <$ RT favors to lie along the [111] axis at RT. This originates from different anisotropies of $DyFe_2$ and $PrFe_2$, whose EMDs lie along the [100] and [111] axes at RT, respectively.[76]

(iv) The XRD patterns for magnetically aligned $Tb_{0.2}Dy_{0.8-x}Pr_x(Fe_{0.9}B_{0.1})_{1.93}$ particles at RT are shown in Fig. 11. The (800) line of the random powders is very weak, but that of the aligned alloys with $0 \leq x < 0.18$ is the strongest peak in their patterns, indicating the [100] EMD. For the alloys with $0.26 \leq x \leq 0.40$, the (400) and (800) peaks are very weak, while the (111)-type peaks are visibly stronger than those for the random powders, indicating the [111] EMD. The intensities of (311), (333), and (800) peaks are comparable for the alloy with $x = 0.22$, suggesting that it has a very small anisotropy at RT.[76]

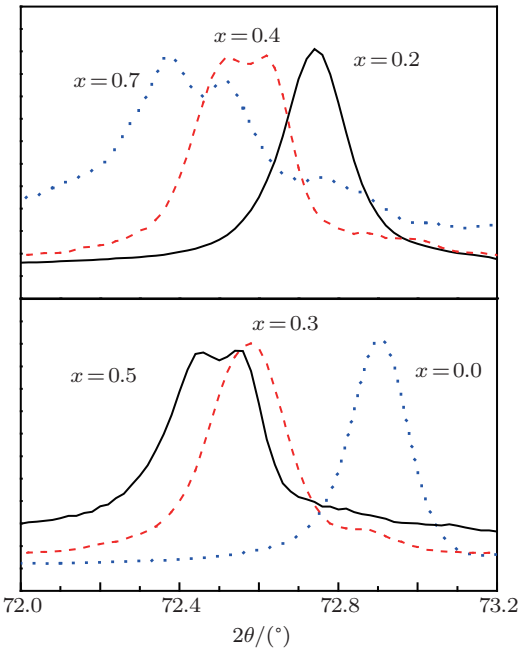


Fig. 10. Profiles of the (440) line of the cubic Laves phase in $Tb_{0.2}Dy_{0.8-x}Pr_x(Fe_{0.9}B_{0.1})_{1.93}$ alloys.[75]

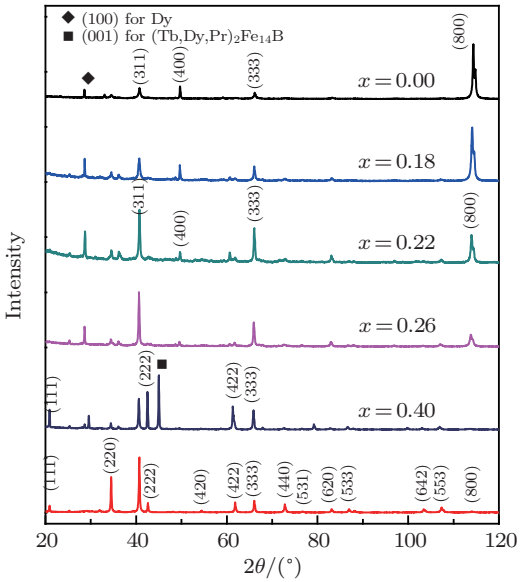


Fig. 11. XRD patterns for magnetically aligned $Tb_{0.2}Dy_{0.8-x}Pr_x(Fe_{0.9}B_{0.1})_{1.93}$ particles at room temperature.[76]

The compensation of anisotropy of Ho^{3+} and Pr^{3+} was proved by Ren *et al.* in $Tb_{0.1}Ho_{0.9-x}Pr_x(Fe_{0.9}B_{0.1})_2$. XRD performed on the magnetically aligned powder shows that the EMD changes from [100] and T_{SR} decreases from high temperature across RT for $x = 0$ to [111] and low temperature for $x = 0.4$. The T_{SR} of the $Tb_{0.1}Ho_{0.7}Pr_{0.2}(Fe_{0.9}B_{0.1})_2$ is 290 K,

very close to RT and that (285 K) of the well known Terfenol-D,[87] and it has the greatest magnetostriction among the alloys with $0 \leq x \leq 0.4$, suggesting a small anisotropy.[78]

The compensation of anisotropy in $Tb_xDy_{0.7-x}Pr_{0.3}(Fe_{0.9}B_{0.1})_{1.93}$ was demonstrated by crystallographic (440) line analysis, T_{SR}, Mössbauer effect, composition-dependence of the anisotropy constant K_1, and magnetostriction. For the compounds with low Tb content, each of the (440) lines is a single peak, suggesting that the EMD lies along [100], while for the compounds with high Tb content, the double splitting of the (440) lines is clearly observed, indicating that the EMD lies along [111]. The temperature dependence of AC initial susceptibility $\chi_{ac}(T)$ of the $Tb_xDy_{0.7-x}Pr_{0.3}(Fe_{0.9}B_{0.1})_{1.93}$ alloys is shown in Fig. 12. The T_{SR} decreases from above 380 K for $x = 0$, 0.13 to 160 K for $x = 0.28$. It means the EMD along [100] for $x < 0.22$ ($T_{SR} >$ RT) and [111] for $x \geq 0.22$ ($T_{SR} <$ RT) at RT.

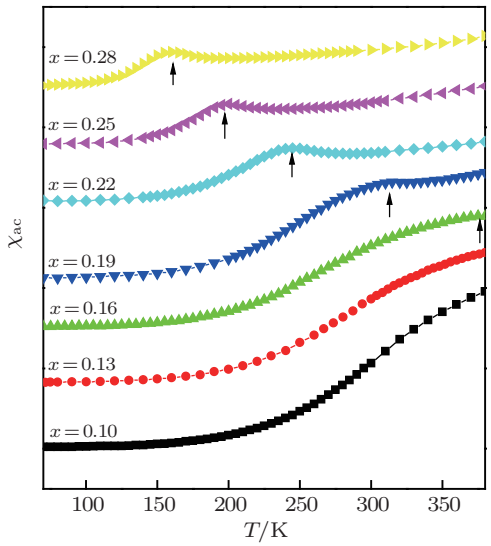


Fig. 12. AC initial susceptibility temperature dependence, $\chi_{ac}(T)$, of the $Tb_xDy_{0.7-x}Pr_{0.3}(Fe_{0.9}B_{0.1})_{1.93}$ alloys (arrow indicates spin reorientation temperature T_{SR}).[88]

The Mössbauer spectrum for the $Tb_{0.15}Dy_{0.55}Pr_{0.3}(Fe_{0.9}B_{0.1})_{1.93}$ alloy shows only one simple six-line subspectra, indicating that the EMD of the Laves phase lies along the ⟨100⟩ axis. The Mössbauer spectrum of the $Tb_{0.25}Dy_{0.45}Pr_{0.3}(Fe_{0.9}B_{0.1})_{1.93}$ alloy can be decomposed into two six-line subspectra with intensity ratio 3:1, which are the characteristics of an EMD along the ⟨111⟩ direction. Figure 13 shows the magnetization curves and magnetocrystalline anisotropy constant K_1 at RT of the $Tb_xDy_{0.7-x}Pr_{0.3}(Fe_{0.9}B_{0.1})_{1.93}$ alloys. Here K_1 is determined from the polycrystalline magnetization curves by using the approach to the saturation magnetization law. It is evident that K_1 minimizes at $x = 0.20$. The composition compensation of anisotropy changes from $x = 0.27$–0.30 for Pr-free $Tb_xDy_{1-x}Fe_2$ to $x = 0.20$ for $Tb_xDy_{0.7-x}Pr_{0.3}(Fe_{0.9}B_{0.1})_{1.93}$, the magnetostriction coefficient λ_{111} at the optimal composition (very near to the composition for the compensation of anisotropy and with EMD lying along [111]) for the latter is 1950 ppm, notably larger than the λ_{111} of 1600 ppm for the former, which has been in widespread practical use.[73,88]

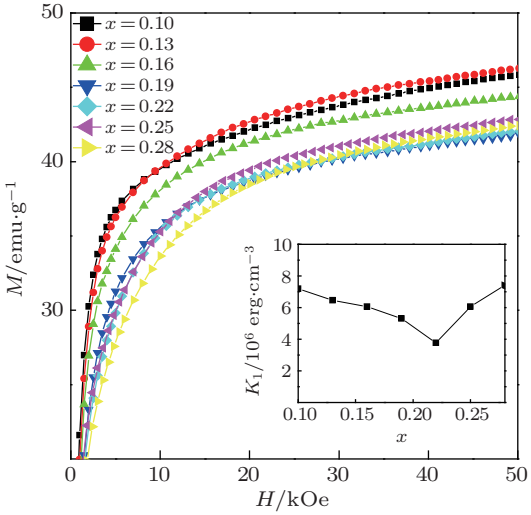


Fig. 13. Magnetization curves and magnetocrystalline anisotropy constant K_1 (inset) at room temperature of the $Tb_xDy_{0.7-x}Pr_{0.3}(Fe_{0.9}B_{0.1})_{1.93}$ alloys.[88]

Measured magnetostriction $\lambda_{\parallel} - \lambda_{\perp}$ under magnetic fields is the resultant action of the magnetostriction coefficient, anisotropy, impurities, and their magnitudes. In RFe_2, λ_{100} is negligible; the anisotropy of the $Tb_{1-x}Pr_xFe_{1.93}B_{0.15}$ is smaller than that of the parent compound $TbFe_{1.93}B_{0.15}$, because the dominant rare-earth anisotropy of Tb^{3+} is larger than that of Pr^{3+}. In the single phase region, the $\lambda_{\parallel} - \lambda_{\perp}$ of $Tb_{1-x}Pr_xFe_{1.93}B_{0.15}$ decreases with increasing Pr content, suggesting that the λ_{111} of $PrFe_2$ is smaller than that of $TbFe_2$, consistent with the conclusion obtained by the XRD crystallographic method.[74] In $Dy_{1-x}Pr_x(Fe_{0.9}B_{0.1})_{1.93}$ alloys, $\lambda_{\parallel} - \lambda_{\perp}$ increases with increasing x in the single phase region of $0 \leq x \leq 0.3$.[77] In the multi-component $Tb_{0.2}Dy_{0.8-x}Pr_x(Fe_{0.9}B_{0.1})_{1.93}$ alloys, as shown in Fig. 14, $\lambda_{\parallel} - \lambda_{\perp}$ increases at the beginning and exhibits a maximum value at $x = 0.22$, and then decreases with further increasing x,[76] a pattern well understood by considering the minimized anisotropy at $x = 0.22$ and the fact that the λ_{111} of $PrFe_2$ is larger than that of $DyFe_2$. In $Tb_{0.1}Ho_{0.9-x}Pr_x(Fe_{0.9}B_{0.1})_{1.93}$ alloys, the result was found to be similar to that in $Tb_{0.2}Dy_{0.8-x}Pr_x(Fe_{0.9}B_{0.1})_{1.93}$ alloys: $\lambda_{\parallel} - \lambda_{\perp}$ increases with x to the composition of $x = 0.2$ with the compensation of anisotropy, and then decreases with further increasing x. It can be concluded that the λ_{111} of $PrFe_2$ is larger than that of $HoFe_2$.[78] In Fig. 15, the $\lambda_{\parallel} - \lambda_{\perp}$ of $Tb_xDy_{0.7-x}Pr_{0.3}(Fe_{0.9}B_{0.1})_{1.93}$ polycrystalline alloys exhibits an additional bulge at $x = 0.2$ in the linear increasing trend with increasing x, agreeing with the report of Clark *et al.*

on $Tb_xDy_{1-x}Fe_2$.[1,8] The bulge position shifts to $x = 0.20$ as the composition for the compensation of anisotropy shifts to there after introducing 30% Pr among the rare-earth.[73] The $Dy_{1-x}Pr_x(Fe_{0.35}Co_{0.55}B_{0.1})_2$ compounds cannot be simply classified as RFe_2 due to the fact that the Co content is more than half of the transition metal. The magnetostrictive attribution of RCo_2 is far from that of RFe_2. RCo_2 possesses large λ_{111} and λ_{100} simultaneously, originating from the rare-earth and Co sublattices, respectively.[72] The composition dependence of magnetostriction involves the competition of the positive λ_{111} of RFe_2 and RCo_2 with the negative λ_{100} of RCo_2. Figure 16 presents the magnetic-field dependence of $\lambda_{\parallel}$ at RT for polycrystalline $Dy_{1-x}Pr_x(Fe_{0.35}Co_{0.55}B_{0.1})_2$ alloys. In the Pr-rich compounds, the EMD lies along [111], while in the Pr-poor ones, the EMD lies along [100]; thus, the magnetostriction is positive and negative in Pr-rich and Pr-poor compounds, respectively.[81]

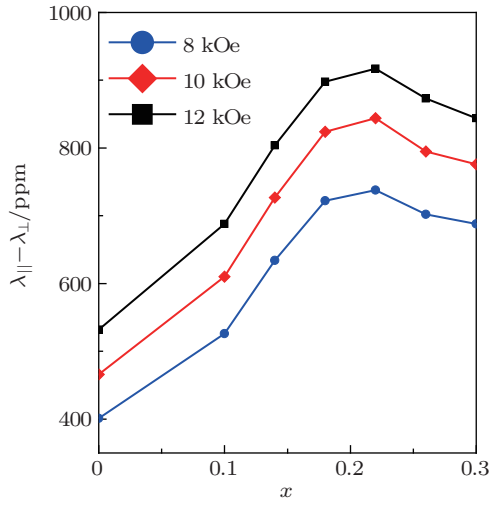


Fig. 14. Magnetostriction $\lambda_{\parallel} - \lambda_{\perp}$ for $Tb_{0.2}Dy_{0.8-x}Pr_x$ $(Fe_{0.9}B_{0.1})_{1.93}$ alloys at different applied magnetic fields.[76]

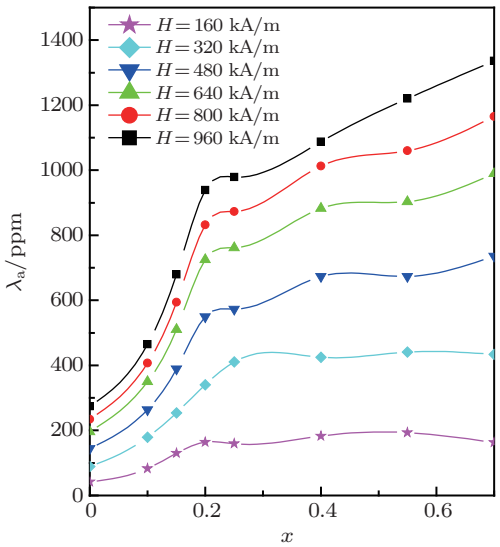


Fig. 15. Magnetostriction $\lambda_{\parallel} - \lambda_{\perp}$ at different applied fields for polycrystalline $Dy_{0.7-x}Tb_xPr_{0.3}$ $(Fe_{0.9}B_{0.1})_{1.93}$ alloys at room temperature.

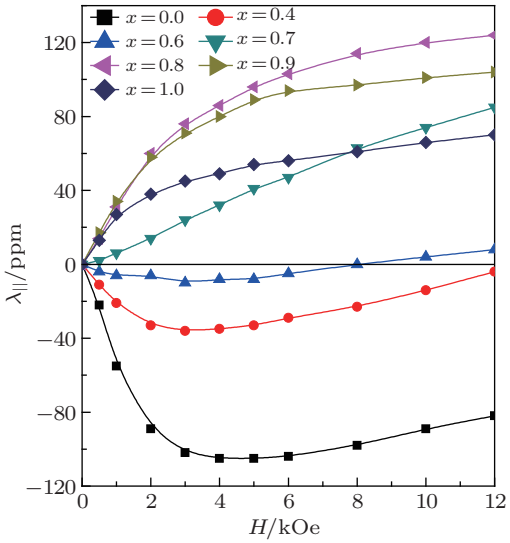


Fig. 16. Magnetic field dependence of $\lambda_{\parallel}$ at room temperature for polycrystalline $Dy_{1-x}Pr_x$ $(Fe_{0.35}Co_{0.55}B_{0.1})_2$ alloys.[81]

RFe_2 Laves compounds containing high Pr content with large magnetostriction may be synthesized by a high-pressure process. The magnetostrictive and anisotropic properties of $PrFe_2$ were clearly addressed by Tang and his colleagues using the samples prepared under high pressure.[89–94] Excellent magnetostrictive property comparable to that of Terfenol-D was found in $Pr_{0.9}Tb_{0.1}Fe_{1.9}$.[89] In $Tb_xPr_{1-x}Fe_{1.9}$ compounds, the normalized $\lambda_{\parallel} - \lambda_{\perp}$ of $Tb_{0.05}Pr_{0.95}(Fe_{0.8}Co_{0.2})_{1.9}$ attains a large value at a relatively weak magnetic field, suggesting much easier saturation, which indicates that this alloy has lower anisotropy than the others, a possible composition for compensation of anisotropy.[90] The $\lambda_{\parallel}$ for $PrFe_{1.9}$ at 5 K and 300 K is 3510 ppm and 920 ppm, respectively, which is extracted from the temperature dependencies of magnetostriction for $Pr_xCe_{1-x}Fe_{1.9}$ in Fig. 17, copied from Ref. [91]. For polycrystalline samples,

$$\lambda_s = \frac{2}{3}(\lambda_{\parallel} - \lambda_{\perp})_{H\to\infty}, \tag{26}$$

$$\lambda_s = \frac{3}{5}\lambda_{111} + \frac{2}{5}\lambda_{100}. \tag{27}$$

Approximately, $\lambda_{\perp} \approx -0.5\lambda_{\parallel}$ when neglecting the magnetostriction contribution of λ_{100} in RFe_2. The λ_{111} of $PrFe_2$ is 5850 ppm and 1530 ppm at 5 K and 300 K, respectively. The former is close to the theoretically calculated value of 5600 ppm at 0 K.[1] The normalized magnetization and $\lambda_{\parallel} - \lambda_{\perp}$ indicate that the composition for compensation of the anisotropy is $Pr_{0.8}Ce_{0.2}Fe_2$.[91] The EMD at RT of $Pr_xNd_{1-x}Fe_{1.9}$ alloys rotates continuously from [100] for $x = 0$ to [111] for $x = 1$, as revealed by the Mössbauer spectra. The composition for the anisotropy compensation was considered to be $x = 0.5$ according to the maximum magnetostriction at low fields of this composition.[92] The composition dependence of magnetostriction $\lambda_{\parallel} - \lambda_{\perp}$ of $Ho_{1-x}Pr_xFe_{1.9}$ displays a maximum and a minimum at $x = 0.2$ and 0.4, respec-

tively. The maximum value corresponds to the compensation of anisotropy, and the minimum one corresponds to the compensation of the magnetization due to the antiparallel alignment of the moments of Ho^{3+} and Pr^{3+}. At the Pr-rich end, the magnetostriction visibly increases with increasing Pr content in accordance with the larger magnetostriction of $PrFe_2$ than $HoFe_2$.[93] Although at RT the EMD of $DyFe_2$ lies along [100] (the same as that of $CeFe_2$, $NdFe_2$, and $HoFe_2$), a direct evidence for the anisotropy compensation between Dy^{3+} and Pr^{3+} ions has not been found in $Dy_{1-x}Pr_xFe_{1.9}$ synthesized at high pressure.[94] The possible reason may come from the much larger anisotropy of Dy^{3+} than that of Ce^{3+}, Nd^{3+}, and Ho^{3+}, the composition for compensation of anisotropy should be very close to $PrFe_2$, e.g., $x > 0.90$, but the experimental composition is absent between 0.9 and 1.0.[93]

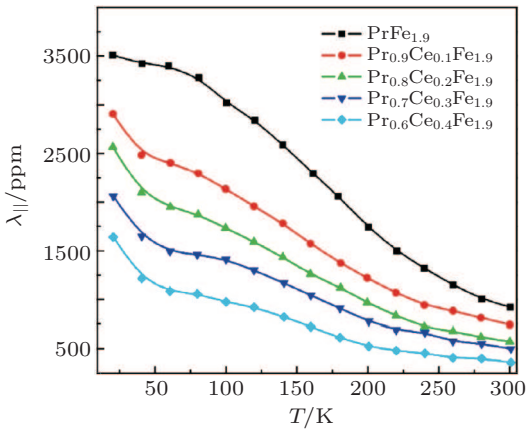


Fig. 17. Temperature dependence of the magnetostriction $\lambda_{\parallel}$ of $Pr_xCe_{1-x}Fe_{1.9}$ at magnetic field of 5 kOe.[91]

3.2.3. Magnetostrictive compounds containing light rare-earth Nd

Like $PrFe_2$, $NdFe_2$ cannot be synthesized at ambient pressure.[83] Guo *et al.* investigated the structure and magnetostriction of $Tb_{1-x}Nd_x(Fe_{0.4}Co_{0.6})_2$ alloys. After Co is introduced, the alloys essentially have the single Laves phase at the entire composition range. The compositions for the compensation of magnetization and anisotropy were determined to be $x = 0.45$ and 0.65, respectively.[95] To eliminate the influence of the Co atoms on the anisotropy and magnetostriction, Ren *et al.* investigated the $Tb_{1-x}Nd_x(Fe_{0.9}B_{0.1})_2$ alloys; however, the single Laves phase was obtained only when $x \leq 0.55$. The complete compensation of magnetocrystalline anisotropy cannot be achieved in this composition range. The magnetostriction coefficient λ_{111} decreases monotonically from 2480 ppm to 1220 ppm when x is increased from 0 to 0.55, indicating that the λ_{111} of the $Nd(Fe,B)_2$ Laves phase is much smaller than that of the $Tb(Fe,B)_2$ Laves phase at RT. Thus, $NdFe_2$ should have a much smaller λ_{111} than $TbFe_2$ at RT.[96] Single Laves phase $Tb_{1-x}Nd_xFe_2$ with $0 \leq x \leq 1$ was synthesized at high pressure. As can be seen in Fig. 18, the Mössbauer spectra of $NdFe_{1.9}$ can be fitted by a single sextet, indicating its EMD along the [100] axis. When x increases to 0.1, the Mössbauer data can be fitted by two sextets with area ratio of about 3:1, which is the characteristic of an EMD along the [111] axis. The deviation of the EMD from [100] to [111] implies that the anisotropy compensation point might be close to $x = 0.1$. The further measurement results of the magnetization and magnetostriction demonstrate the composition for the compensation of anisotropy.[97] The Laves compound contains additional light rare-earth, e.g., Pr or Sm, and some Nd settled in the Pr or Sm part.

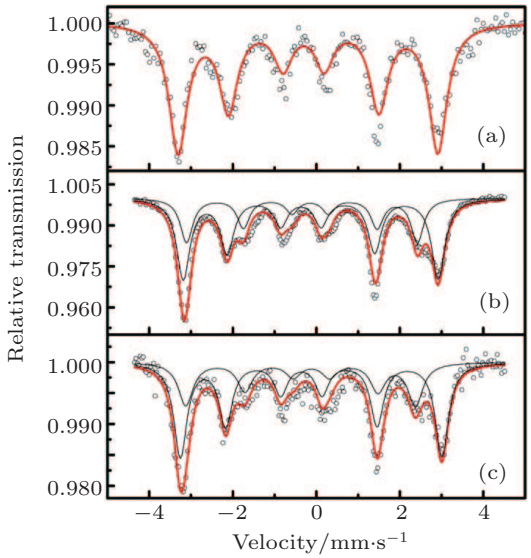


Fig. 18. Mössbauer spectra at room temperature for $Tb_xNd_{1-x}Fe_{1.9}$ alloys ((a) $x = 0.0$, (b) $x = 0.1$, (c) $x = 0.2$).[97]

3.2.4. Magnetostrictive compounds containing light rare-earth Sm

$SmFe_2$ has a large but negative magnetostriction that is comparable with the largest RT magnetostriction known to date of $TbFe_2$. Its single crystal was first grown by Samata *et al.* in 1998.[98] The magnetostriction was measured to be -2040 ppm at RT, quite consistent with that obtained from the XRD method performed on a polycrystalline sample. The EMD lies along [110] at low temperature and changes to [111] above 195 K. Therefore, $SmFe_2$ has a relatively small K_1 of -5.3×10^6 erg/cm^3 at RT, an order smaller than that of $TbFe_2$ and $DyFe_2$.[99] However, the K_1 of $SmFe_2$ is an order larger than that ($-(0.4$–$0.6)\times 10^6$ erg/cm^3) of the practical Terfenol-D, in which the EMD changes from [100] to [111] at 283–285 K.[8,87,100] To reduce the anisotropy and maintain the large magnetostriction of $SmFe_2$, RFe_2 with a large negative magnetostriction and a positive anisotropy should be used to alloy $(Sm,R)Fe_2$. $YbFe_2$ is such a unique compound.[1] However, $YbFe_2$ can be synthesized only under high pressure,[1,83] the magnetostriction and anisotropy data at RT have not been reported to date. Guo *et al.* investigated the magnetostriction of the pseudobinary compounds $Sm_{1-x}Yb_xFe_2$: a

slight enhancement in magnetostriction has been found when $x = 0.05$, but the complete compensation of anisotropy has not been reached.[101] A possible reason is that the anisotropy of $YbFe_2$ is not large enough and that the single-phase $Sm_{1-x}Yb_xFe_2$ compounds with high Yb content are not obtainable. Therefore, one has to alloy $SmFe_2$ with an RFe_2 compound with large positive anisotropy and smaller positive magnetostriction.[1,84,102–105,108] In $Sm_{1-x}Dy_xFe_2$, $SmFe_2$ and $DyFe_2$ contribute negative and positive magnetostrictions, respectively. But the absolute value of the positive K_1 of $DyFe_2$ is one order larger than that of negative K_1 of $SmFe_2$. This suggests that the composition for anisotropy compensation is very close to $SmFe_2$, thus, the counteraction of the magnetostriction is small, and a large magnetostriction remains. $Sm_{1-x}Dy_xFe_2$ with $x = 0.10$–0.15, known as Samfenol-D, was constructed. It possesses excellent magnetostrictive properties comparable to those of Terfenol-D.[1,84,102] A Mössbauer effect study at RT indicated that the EMD of $Sm_{1-x}Dy_xFe_2$ compounds lies along [111] when $x < 0.15$ and along [100] when $x > 0.4$. The composition for compensation of the anisotropy is $x = 0.15$, where $\lambda_{\parallel} - \lambda_{\perp}$ is 1524 ppm.[103] RFe_2 with positive magnetostriction smaller than $DyFe_2$ is more beneficial to the reduction of the counteraction of magnetostriction. $NdFe_2$ and $CeFe_2$ have the same anisotropy sign as $DyFe_2$, but much smaller positive magnetostriction.[57] Hari Badu *et al.* investigated the magnetostrictive properties of $Sm_{1-x}Nd_xFe_{1.93}$. A polycrystalline magnetostriction of $\lambda_{\parallel} = -1572$ ppm and $\lambda_{\parallel} - \lambda_{\perp} = -2220$ ppm were found and shown in Fig. 19 for $Sm_{0.88}Nd_{0.12}Fe_{1.93}$.[104] Further detailed investigations were performed by Wang *et al.*[105] The thermomagnetic curves of $Sm_{1-x}Nd_xFe_2$ alloys show that the T_{SR} of $Sm_{1-x}Nd_xFe_2$ gradually increases from 195 K for $x = 0$ to 270 K for $x = 0.30$. The T_{SR} of $Sm_{1-x}Nd_xFe_2$ monotonously approaches RT with increasing x, suggesting that, at RT, the anisotropy of the compounds decreases with increasing Nd content. Considering that T_{SR} of the anisotropy-compensated Terfenol-D is ~ 285 K, very close to RT,[87,100] the lower T_{SR} of $Sm_{1-x}Nd_xFe_2$ suggests that the anisotropy at RT has not reached the minimum value even for $x = 0.30$. The temperature dependence of the magnetostriction $\lambda_{\parallel}$ of $Sm_{1-x}Nd_xFe_2$ at 6 kOe, and that of $Sm_{0.88}Nd_{0.12}Fe_2$ at 2 kOe, 4 kOe, and 6 kOe are presented in Figs. 20(a) and 20(b), respectively. The $\lambda_{\parallel}$ exhibits a maximum at the respective T_{SR}'s of the compounds due to the minimum anisotropy at T_{SR}, which is similar to the temperature dependencies of magnetostriction for (Tb, Dy)Fe_2 and (Tb, Dy, Ho)Fe_2 compounds.[16] The quasi-static piezomagnetic coefficient d_{33} of the $Sm_{1-x}Nd_xFe_2$ compounds was measured with a sinusoidal magnetic drive field (H_3) of 200 Oe (amplitude) at 0.1 Hz at various magnetic bias fields H_{bias} (Fig. 21). For each compound, the d_{33} vs. H_{bias} curve exhibits a broad maximum, which is related to the saturation magnetostriction and decreases with increasing Nd concentration. Although $Sm_{0.88}Nd_{0.12}Fe_2$ has a smaller saturation magnetostriction than $SmFe_2$, its d_{33} at H_{bias} smaller than 0.5 kOe is larger than that of $SmFe_2$ due to the compensation of anisotropy. The optimal H_{bias}, where d_{33} has a maximum, decreases from 800–900 Oe for $SmFe_2$ to 700 Oe for $Sm_{0.88}Nd_{0.12}Fe_2$. The optimal H_{bias} of 700 Oe for $Sm_{0.88}Nd_{0.12}Fe_2$ is very close to the value of about 500 Oe usually used for Terfenol-D. The maximum value of d_{33} for $Sm_{0.88}Nd_{0.12}Fe_2$ is 0.55 ppm/Oe (6.8 nm/A), which

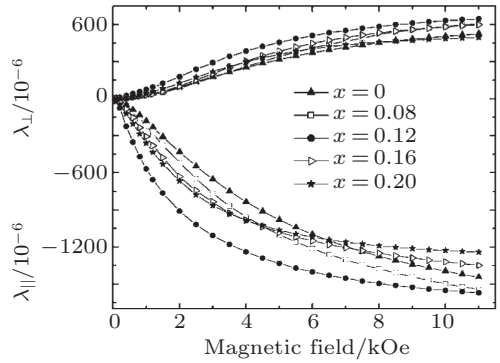


Fig. 19. Magnetostriction curves of $Sm_{1-x}Nd_xFe_{1.93}$ compounds at room temperature.[104]

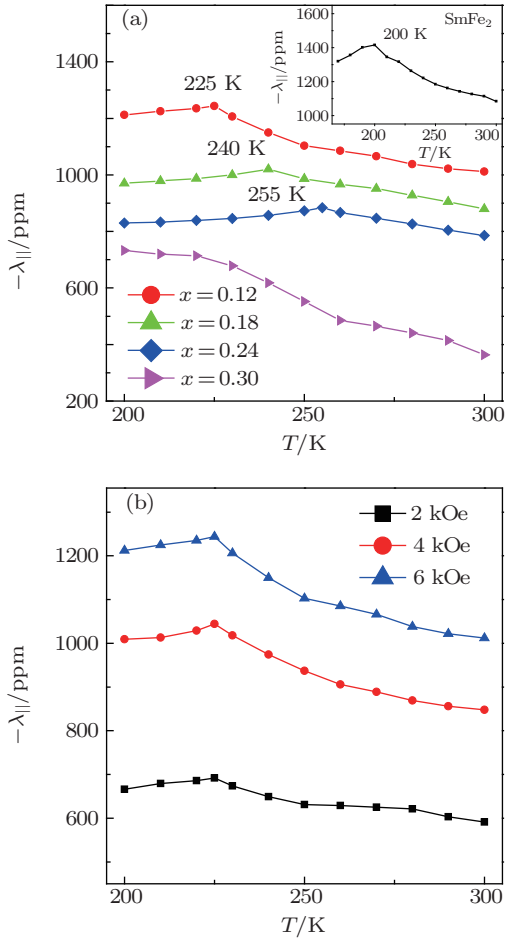


Fig. 20. Temperature dependence of the static magnetostriction $\lambda_{\parallel}$ of (a) $Sm_{1-x}Nd_xFe_2$ at 6 kOe and (b) $Sm_{0.88}Nd_{0.12}Fe_2$ at applied fields of 2 kOe, 4 kOe, and 6 kOe.[105]

is a value with promising prospect for polycrystalline magnetostrictive materials without stress bias, compared with the value (less than 0.80 ppm/Oe (10 nm/A)) for polycrystalline Terfenol-D without stress bias.[106,107] Magnetostriction and magnetic anisotropy of (Sm, Ce)Fe_2 compounds were investigated by Ren *et al.* It was found that the anisotropy at RT of $Sm_{1-x}Ce_xFe_2$ decreases with increasing Ce content due to the anisotropy compensation between Sm and Ce ions. Thus, a small amount of Ce substitution for Sm in $SmFe_2$ improves the magnetostriction $\lambda_{\parallel}$ at low magnetic fields, but the intensity of the improvement is limited.[108] In $Sm_{1-x}Pr_xFe_2$ compounds, the magnetostriction $-(\lambda_{\parallel}-\lambda_{\perp})$ of $Sm_{0.9}Pr_{0.1}Fe_2$ was found to be larger than that of $SmFe_2$, since $PrFe_2$ has a large positive magnetostriction opposite to the negative one of $SmFe_2$, the magnetostriction increment of the Pr-substituted compounds was ascribed to the compensation of anisotropy between Sm^{3+} and Pr^{3+}.[109,110]

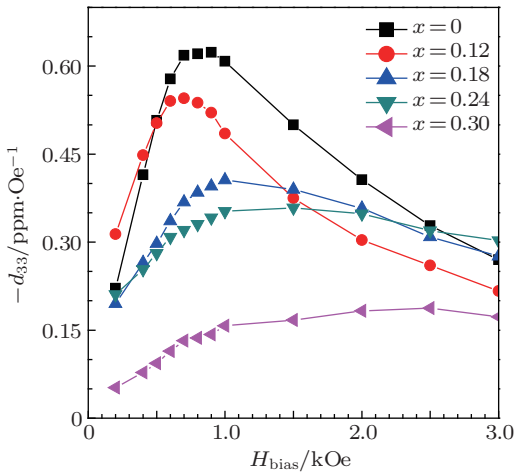


Fig. 21. Dependence of d_{33} of $Sm_{1-x}Nd_xFe_2$ compounds at room temperature on $H_{\rm bias}$ at 0.1 Hz.[105]

Considerable efforts have been made to investigate the substitution effect on magnetic and magnetostrictive properties in (Sm, *R*)$(Fe_{1-x}TM_x)_2$ (*R* = Dy, Pr, Nd and *TM* = Co, Ni, Mn, Al, ...) cubic Laves phase compounds.[111–115] In the (Sm, *R*)$(Fe_{1-x}Co_x)_2$ compounds with *R* = Dy, Pr, Nd,[111–113] T_C and M_s display peaks at about $x = 0.2$ in every case, which is very similar to the composition dependencies of T_C and M_s for $Tb_{0.27}Dy_{0.73}(Fe_{1-x}Co_x)_2$ compounds,[17,19,24] implying the same origin in the transition-metal sublattice. In fact, in Slater–Pauling curves, T_C and M_s of $Fe_{1-x}Co_x$ alloy both obtain maximum values at $x \approx 0.33$, the deviation of the composition of 0.13 comes from the very dilute experimental compositions in these systems. However, the trend of λ_{111} depending on the composition for (Sm, *R*)$(Fe_{1-x}Co_x)_2$ does not obey the weighted stacking law, unlike the $Tb_{0.36}Dy_{0.64}(Fe_{1-x}Co_x)_2$ compounds.[117] The λ_{111} of (Sm, *R*)$(Fe_{1-x}Co_x)_2$ slightly increases when $x \leq 0.4$, and bulges when $0.6 \leq x \leq 0.8$, with increasing Co substitution for Fe. The $|\lambda_{\parallel}-\lambda_{\perp}|$ decreases with increasing *x*. From the $|\lambda_{\parallel}-\lambda_{\perp}|$ at high magnetic fields, by using the approach-to-saturation law, the saturation magnetostriction λ_s can be obtained by Eq. (1). Furthermore, λ_{100} is obtained by Eq. (27). In these compound systems, the composition dependencies of λ_{100} and $-\lambda_{111}$ are very similar. Due to the small $|\lambda_{\parallel}-\lambda_{\perp}|$, the value of λ_{100} is comparable to that of λ_{111} but with the opposite sign. For instance, the composition dependences of spontaneous magnetostriction λ_{111}, λ_{100} and saturation magnetostriction λ_s of $Sm_{0.9}Pr_{0.1}(Fe_{1-x}Co_x)_2$ are shown in Fig. 22. As is well known, great anisotropic magnetostriction $\lambda_{111} \gg \lambda_{100}$ is a typical characteristic of the RFe_2 compounds. The very small λ_{100} originates from the Fe sublattice, while in RCo_2 compounds, λ_{100} may reach as large as 2200 ppm duo to the contribution from the Co sublattice.[72] Thus, it is reasonable for a $R(Fe,Co)_2$ compound to possess a large λ_{100}. Attention should be paid to the magnitudes of λ_{111}, which are −2520 ppm, −4600 ppm, and −4020 ppm for $Sm_{0.9}R_{0.1}(Fe_{0.4}Co_{0.6})_2$ with *R* = Dy, Pr, and Nd, respectively. These values, especially for *R* = Pr and Nd, are much larger than the largest known λ_{111} of 2460 ppm for $TbFe_2$, and −2040 ppm for the parent compound $SmFe_2$. This means that the λ_{111} of $Sm_{0.9}R_{0.1}(Fe_{1-x}Co_x)_2$ cannot be well comprehended by the RFe_2 magnetostriction theory under the frame of rare-earth single-ion approach. $Tb(Fe_{1-x}Co_x)_2$ and $Tb_{0.27}Dy_{0.73}(Fe_{1-x}Co_x)_2$ were investigated in 1970s. No λ_{111} peak was reported at $x = 0.6$–0.8, their λ_{111} can be well understood as originating from the contribution of rare-earth, and the Fe–Co sublattice contributes only to λ_{100} not to λ_{111}. If this conclusion can also be applied to $Sm_{0.9}R_{0.1}(Fe_{1-x}Co_x)_2$, the presence of Sm might be the most critical factor for the large λ_{111}. As is known, in these studies, λ_{111} was obtained by investigating the structural distortion using the XRD method. The premise of this method is to consider the entire distortion caused by magnetostriction, excluding the influence of mechanical strain, texture, and so forth. Unfortunately, Mushnikov *et al.* found induced crystal structural distortions in $Sm(Fe_{1-x}Co_x)_2$ compounds after samples absorbed a small quantity of hydrogen from the atmosphere under normal conditions. The crystal lattice distortion parameter ε in the original paper is the same as $\Delta\alpha$ in Section 2.1 of this paper, which was proved to equate to λ_{111} and obtained by the same XRD method. The ε of $Sm(Fe_{1-x}Co_x)_2H_n$ (*n* is a parameter for H content) has a maximum in the Co-rich part of the composition range at $x = 0.6$, and the maximum value reaches 6000 ppm (Fig. 4 in Ref. [118]). The ε dependence on the Co content of the hydrogen-absorbed compound very much resembles the behavior of the λ_{111} of $Sm_{0.9}R_{0.1}(Fe_{1-x}Co_x)_2$. Since it is hard to prevent hydrogen absorption in these compounds, determining the proportion of the total distortion originating from magnetostriction is currently impossible. A direct magnetostriction measurement along the different directions of a

single crystal may be the way to determine whether extra large magnetostriction occurs. Mn or Al is non-magnetic in the Mn- or Al-substituted (SmR)Fe_2 compounds, while the moments of rare-earth and transition metal align in parallel. The Mn or Al substitution weakens the interaction of Fe–Fe and R–Fe, therefore leading to a decrease of both Curie temperature and magnetization. It also disturbs the Fe sublattice, which induces decreases of the magnetostriction coefficient and magnetostriction $\lambda_{\parallel} - \lambda_{\perp}$ with the increase of Mn or Al substitution for Fe.[114–116]

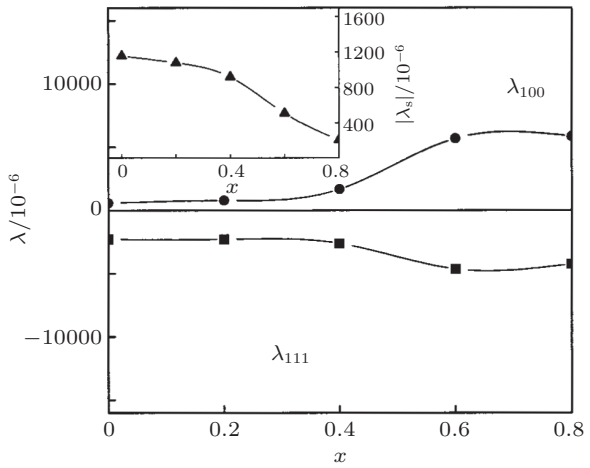


Fig. 22. Composition dependence of spontaneous magnetostriction λ_{111}, λ_{100} and saturation magnetostriction λ_s (inset) of $Sm_{0.9}Pr_{0.1}(Fe_{1-x}Co_x)_2$.[112]

4. Summary and outlook

We have reviewed the recent progress in understanding the bulk magnetostrictive Laves phase, especially with regard to the magnetostriction and the minimization of the anisotropy of the light rare-earth-based compounds. Some of the important results are summarized briefly as follows. A small amount of ($\sim$ 20%) Co substituted for Fe in Terfenol-D may increase magnetostriction coefficient λ_{100}. Increasing Tb content increases λ_{111}, but only these two cases concur, e.g. $Tb_{0.3-0.36}Dy_{0.7-0.64}(Fe_{0.8}Co_{0.2})_2$, the small anisotropy and excellent properties of Terfenol-D remain. Under the stability of a small amount of boron, 30% Pr may be substituted for the expensive heavy rare-earth in Terfenol-D, which may lead to a significant decrease in the cost while keeping the excellent magnetostrictive properties. To further decrease the cost, poor or free of heavy rare-earth magnetostrictive materials with excellent properties may develop in Sm-based RFe$_2$ compounds. Extra large magnetostriction may exist in (SmR)$(Fe_{1-x}Co_x)_2$ compounds, but needs to be confirmed by single crystal growth and direct magnetostriction measurement. The magnetostriction coefficient λ_{111} of $RR'Fe_2$ obeys the weighted stacking rule. The magnetic anisotropy of Pr^{3+} and Sm^{3+} ions was discovered to be the opposite of that of Dy^{3+}, Ho^{3+}, Nd^{3+}. The anisotropy constant K_1 of $RR'Fe_2$ almost obeys the linear rule. When K_1 for either R or R' is not available, the element and composition dependence of the spin reorientation temperature is a good replacement, which may be used to design a magnetostrictive material with small anisotropy.

For further investigation in this field, we propose the following directions.

1) Sm-based RFe$_2$ compounds. Sm-based compounds have excellent magnetostrictive properties (possibly with extra large magnetostriction), and have a great price advantage over Terfenol-D. Investigations of microstructure, stress, and frequency dependencies of magnetostrictive and magnetoelastic properties and magnetostriction hysteresis in these compounds are urgently needed. To grow single crystals or [111]/[100] aligned samples for study is the top priority.

2) RFe$_2$ compounds with EMD along [100]. While the magnetostriction of TbFe$_2$ and SmFe$_2$ with EMD along [111] can be well interpreted by the single-ion approach and large anisotropy of magnetostriction $\lambda_{111} \gg \lambda_{100}$, the magnetostriction of DyFe$_2$, HoFe$_2$, etc., with EMD along [100], simply could not be well understood so far. Although the magnetostriction of these compounds is not so large, their investigation has theoretical significance.

3) The action of transition-metal sublattice. Large magnetostriction λ_{111} and anisotropy of magnetostriction $\lambda_{111} \gg \lambda_{100}$ in RFe$_2$ and RR'Fe$_2$ compounds with pure Fe sublattice can be explained based on the structure of the Laves phase and the rare-earth sublattice, and the contribution of the Fe sublattice may be neglected. However, the magnetostriction λ_{111} usually decreases when other metals are substituted for Fe. And the large anisotropy of magnetostriction simply cannot occur in isostructural RCo$_2$ compounds. The action and the interplay with the rare-earth sublattice of the transition-metal sublattice might be further addressed, especially at a basic physics level, for instance, by first-principles study.

References

[1] Clark A E 1980 *Handbook of Ferromagnetic Materials* (Wohlfarth E P, ed.) (Amsterdam: Elsevier) Vol. **1** p. 531
[2] Summers E M, Lograsso T A and Wun-Fogle M 2007 *J. Mater. Sci.* **42** 9582
[3] Söderberg O, Sozinov A, Ge Y, Hannula S P and Lindroos V K 2006 *Handbook of Magnetic Materials* (Buschow K H J, ed.) (Amsterdam: Elsevier) Vol. **16** p. 1
[4] Trudel S, Gaier O, Hamrle J and Hillebrands B 2010 *J. Phys. D: Appl. Phys.* **43** 193001
[5] Darnell F J 1963 *Phys. Rev.* **132** 128
[6] Legvold S, Alstad J and Rhyne J 1963 *Phys. Rev. Lett.* **10** 509
[7] Clark A E and Belson H S 1972 *Phys. Rev. B* **5** 3642
[8] Clark A E 1974 *AIP Conf. Proc.* **18** 1015
[9] Clark A E, Teter J P and Mcmasters O D 1988 *J. Appl. Phys.* **63** 3910
[10] Koon N C, Williams C M and Das B N 1991 *J. Magn. Magn. Mater.* **100** 173
[11] Andreev A V 1995 *Handbook of Magnetic Materials* (Buschow K H J, ed.) (Amsterdam: Elsevier) Vol. **8** p. 59
[12] Jiles D C 1994 *J. Phys. D: Appl. Phys.* **27** 1

[13] Yang S, Bao, H X, Zhou C, Wang Y, Ren X B, Matsushita Y, Katsuya Y, Tanaka M, Kobayashi K, Song X P and Gao J R 2010 *Phys. Rev. Lett.* **104** 197201
[14] Dwight A E and Kimball C W 1974 *Acta Crystallogr. B* **30** 2791
[15] Williams C and Koon N 1977 *Physica B+C* **86–88** 147
[16] Restorff J B, Wun-Fogle M and Clark A E 2000 *J. Appl. Phys.* **87** 5786
[17] Clark A E, and Teter J P and McMasters O D 1987 *IEEE Trans. Magn.* **23** 3526
[18] Teter J P, Clark A E, Wunfogle M and McMasters O D 1990 *IEEE Trans. Magn.* **26** 1748
[19] Clark A E, and Teter J P and Wun-Fogle M 1991 *J. Appl. Phys.* **69** 5771
[20] Funayama T, Kobayashi T, Sakai I and Sahashi M 1992 *Appl. Phys. Lett.* **61** 114
[21] Guo H Q, Yang H Y, Shen B G, Yang L Y and Li R Q 1993 *J. Alloys Compd.* **190** 255
[22] Prajapati K, Jenner A G and Greenough R D 1993 *IEEE Trans. Magn.* **29** 3514
[23] Mohan C V 1996 *J. Alloys Compd.* **238** 86
[24] Dhilsha K R and Rama Rao K V S 1993 *J. Appl. Phys.* **73** 1380
[25] Kobayashi T, Sasaki I, Funayama T and Sahashi M 1994 *J. Appl. Phys.* **76** 7024
[26] Prajapati K, Jenner A G and Greenough R D 1995 *IEEE Trans. Magn.* **31** 3976
[27] Senthil Kumar M, Reddy K V and Rama Rao K V S 1995 *J. Appl. Phys.* **77** 4589
[28] Youhui G, Zhu J H and Tai L C 1996 *J. Magn. Magn. Mater.* **152** 379
[29] Mei W, Okane T and Umeda T 1997 *J. Alloys Compd.* **248** 132
[30] Wu L, Zhan W S and Chen X C 1997 *J. Alloys Compd.* **255** 236
[31] Zhang H P, Zhu H Q and Du T 1997 *J. Alloys Compd.* **258** 20
[32] Shi Z X, Chen Z M, Wang X H, Lin M H and Zhang Y M 1997 *J. Alloys Compd.* **258** 30
[33] Liu J J, Ren W J, Li D, Sun N K, Zhao X G, Li J and Zhang Z D 2007 *Phys. Rev. B* **75** 064429
[34] Ma T Y, Jiang C B and Xu H B 2005 *Appl. Phys. Lett.* **86** 162505
[35] Ma T Y, Jiang C B, Xu X, Zhang H and Xu H B 2005 *J. Magn. Magn. Mater.* **292** 317
[36] Ma T Y, Yan M, Zhang C S, Pei Y M and Jiang C B 2009 *J. Appl. Phys.* **105** 093915
[37] Ma T Y, Jiang C B, Xiao F and Xu H B 2006 *J. Alloys Compd.* **414** 276
[38] Ma T Y, Yan M, Zhang J J, Luo W, Jiang C B and Xu H B 2007 *Appl. Phys. Lett.* **90** 102502
[39] Jiang C B, Ma T Y and Xu H B 2008 *J. Alloys Compd.* **449** 156
[40] Verhoeven J D, Gibson E D, McMasters O D and Baker H H 1987 *Metall. Trans. A* **18** 223
[41] Zhao Y, Jiang C B, Zhang H and Xu H B 2003 *J. Alloys Compd.* **354** 263
[42] Wu G H, Zhao X G, Wang J H, Li J Y, Jia K C and Zhan W S 1995 *Appl. Phys. Lett.* **67** 2005
[43] Zhao X G, Wu G H, Wang J H, Jia K C and Zhan W S 1996 *J. Appl. Phys.* **79** 6225
[44] Du J, Wang J H, Tang C C, Li Y X, Wu G H and Zhan W S 1998 *Appl. Phys. Lett.* **72** 489
[45] Chen F M, Fang J S and Chin T S 1996 *IEEE Trans. Magn.* **32** 4776
[46] Shih J C, Chin T S, Chen C A and Fang J S 1999 *J. Magn. Magn. Mater.* **191** 101
[47] Wu L, Zhan W S, Chen X C and Chen X S 1995 *J. Magn. Magn. Mater.* **139** 335
[48] Ren W J, Zhang Z D, Markosyan A S, Zhao X G, Jin X M and Song X P 2001 *J. Phys. D: Appl. Phys.* **34** 3024
[49] Ren W J, Zhang Z D, Liu J P, Zhao X G, Liu W, Geng D Y and Jin X M 2002 *J. Appl. Phys.* **91** 8207
[50] Wun-Fogle M, Restorff J B, Clark A E and Lindberg J F 1998 *J. Appl. Phys.* **83** 7279
[51] Wun-Fogle M, Restorff J B and Clark A E 1999 *J. Appl. Phys.* **85** 6253
[52] Jiang C B, Zhang H B, Wang Z B and Xu H B 2008 *J. Phys. D: Appl. Phys.* **41** 155012
[53] Zhang Z B, Liu J H, Jiang C B and Xu H B 2011 *J. Appl. Phys.* **109** 123923
[54] Prajapati K, Jenner A G, Schulze M P and Greenough R D 1993 *J. Appl. Phys.* **73** 6171
[55] Xu L H, Jiang C B and Xu H B 2006 *Appl. Phys. Lett.* **89** 192507
[56] Xu L H, Jiang C B, Zhou C G and Xu H B 2008 *J. Alloys Compd.* **455** 203
[57] Franse J J M and Radwański R J 1993 *Handbook of Magnetic Materials* (Buschow K H J, ed.) (Amsterdam: Elsevier) Vol. **7** p. 307
[58] Tang C C, Zhan W S, Li Y X, Chen D F, Du J, Wu G H, Li J Y and Jia K C 1997 *J. Phys.: Condens. Matter* **9** 9651
[59] Tang C C, Chen D F, Li Y X, Wu G H, Jia K C and Zhan W S 1997 *J. Appl. Phys.* **82** 4424
[60] Tang C C, Zhan W S, Chen D F, Li Y X, Du J, Shen B G and Wu G H 1998 *J. Phys.: Condens. Matter* **10** 2797
[61] Tang C C, Zhan W S, Li Y X, Chen D F, Du J, Wu G H, Gan Z W and Qi S R 1998 *J. Phys. D: Appl. Phys.* **31** 2426
[62] Shimotomai M, Miyake H and Doyama M 1980 *J. Phys. F: Met. Phys.* **10** 707
[63] Zhao X G, Li J Y, Liu S C, Ji S Q and Jia K C 1997 *J. Alloys Compd.* **258** 39
[64] Wu C H, Yang C P, Chuang Y C, Jin X M and Li J Y 1997 *J. Magn. Magn. Mater.* **166** 249
[65] Wang B W, Wu C H, Deng W, Tang S L, Jin X M, Chuang Y C and Li J Y 1996 *J. Appl. Phys.* **79** 2587
[66] Tang S L, Wu C H, Jin X M, Wang B W, Chuang Y C, Li J Y and Zhao X G 1997 *J. Alloys Compd.* **256** 247
[67] Gschneidner Jr K A 1985 *J. Less-Common. Met.* **114** 29
[68] Guo Z J, Wang B W, Zhang Z D, Zhao X G, Jin X M, Liu W and Xiao Q F 1997 *Appl. Phys. Lett.* **71** 2836
[69] Wang B W, Guo Z J, Zhang Z D, Zhao X G and Busbridge S C 1999 *J. Appl. Phys.* **85** 2805
[70] Liu J J, Ren W J, Shen S L, Li D, Li J, Zhao X G, Liu W and Zhang Z D 2006 *J. Phys. D: Appl. Phys.* **39** 243
[71] Guo Z J, Busbridge S C, Wang B W, Zhang Z D and Zhao X G 2001 *IEEE Trans. Magn.* **37** 3025
[72] Levitin R Z and Markosyan A S 1990 *J. Magn. Magn. Mater.* **84** 247
[73] Ren W J, Zhang Z D, Zhao X G, Liu W and Geng D Y 2004 *Appl. Phys. Lett.* **84** 562
[74] Ren W J, Zhang Z D, Zhao X G, Song X P, Liu W and Geng D Y 2004 *J. Magn. Magn. Mater.* **269** 281
[75] Ren W J, Zhang Z D, Song X P, Zhao X G and Jin X M 2003 *Appl. Phys. Lett.* **82** 2664
[76] Ren W J, Liu J J, Li D, Liu W, Zhao X G and Zhang Z D 2006 *Appl. Phys. Lett.* **89** 122506
[77] Ren W J, Zhang Z D, Zhao X G, You C Y and Geng D Y 2003 *J. Alloys Compd.* **359** 119
[78] Ren W J, Li D, Liu W, Li J and Zhang Z D 2008 *J. Appl. Phys.* **103** 07B311
[79] Liu JJ, Ren W J, Li J, Zhao X G, Liu W and Zhang Z D 2005 *Appl. Phys. Lett.* **87** 082506
[80] Liu JJ, Ren W J and Zhang Z D 2008 *J. Phys. D: Appl. Phys.* **41** 125003
[81] Ren W J, Li D, Sui Y C, Liu W, Zhao X G, Liu J J, Li J and Zhang Z D 2006 *J. Appl. Phys.* **99** 08M701
[82] Lv X K, Liu W, Ren W J, Li B, Zhao X G, Li D and Zhang Z D 2008 *J. Magn. Magn. Mater.* **320** 2373
[83] Meyer C, Hartmann-Boutron F, Gros Y, Berthier Y and Buevoz J L 1981 *J. Phys. (France)* **42** 605
[84] Clark A E, Abbundi R, McMasters O and Savage H 1977 *Physica B+C* **86–88** 73
[85] Clark A E, Cullen J R, McMasters O and Callen E 1976 *AIP Conf. Proc.* **29** 192
[86] Tang Y J, Wu C H, Zhong X P and Luo X L 1993 *Phys. Stat. Sol. (a)* **140** 231
[87] Sato K, Isikawa Y, Mori K, Clark A E and Callen E 1986 *J. Magn. Magn. Mater.* **54–57** 875
[88] Liu J J, Ren W J, Zhang Z D, Li D, Li J, Zhao X G, Liu W and Or S W 2006 *J. Appl. Phys.* **100** 023904
[89] Shi Y G, Tang S L, Wang R L, Su H L, Han Z D, Lv L Y and Du Y W 2006 *Appl. Phys. Lett.* **89** 202503
[90] Shi Y G, Tang S L, Yu J Y, Zhai L Zhang X K, Du Y W and Yang C P 2009 *J. Appl. Phys.* **105** 07A925
[91] Wang Y, Zhai L, Shi Y G, Tang S L and Du Y W 2010 *J. Appl. Phys.* **107** 103902
[92] Shi Y G, Zhai L, Tang S L and Chen R J 2011 *J. Appl. Phys.* **109** 07A915
[93] Shi Y G, Zhai L, Wang Y, Fan J Y, Shi D N, Tang S L and Du Y W 2012 *J. Magn. Magn. Mater.* **324** 1627

[94] Shi Y G, Tang S L, Lv L Y and Fan J Y 2010 *J. Alloys Compd.* **506** 533
[95] Guo Z J, Busbridge S C, Wang B W, Zhang Z D, Zhao X G and Geng D Y 1999 *J. Appl. Phys.* **86** 6310
[96] Ren W J, Or S W, Chan H L W, Zhao X G, Liu J J and Zhang Z D 2004 *IEEE Trans. Magn.* **40** 2772
[97] Shi Y G, Tang S L, Huang Y J, Lv L Y and Du Y W 2007 *Appl. Phys. Lett.* **90** 142515
[98] Samata H, Fujiwara N, Nagata Y, Uchida T and Lan M D 1998 *Jpn. J. Appl. Phys.* **37** 5544
[99] Samata H, Fujiwara N, Nagata Y, Uchida T and Lan M D 1999 *J. Magn. Magn. Mater.* **195** 376
[100] Abbundi R and Clark A E 1977 *IEEE Trans. Magn.* **13** 1519
[101] Guo Z J, Zhang Z D, Busbridge S C, Wang B W, Zhao X G and Geng D Y 2001 *J. Magn. Magn. Mater.* **231** 191
[102] Abbundi R, Clark A E and McMasters O D 1982 *J. Appl. Phys.* **53** 2664
[103] Guo H Q, Yang H Y, Gong H Y, Yang L Y, Shen B G and Li R Q 1994 *J. Appl. Phys.* **75** 7429
[104] Hari Badu V, Markandeyulu G and Subrahmanyam A 2006 *Appl. Phys. Lett.* **90** 252513
[105] Wang Y, Ren W J, Yang Y H, Li B, Li J and Zhang Z D 2013 *J. Appl. Phys.* **113** 143903
[106] Kendall D and Piercy A R 1990 *IEEE Trans. Magn.* **26** 1837
[107] Jenner A G, Greenough R D, Wilkinson A J and Parvinmehr A 1990 *IEEE Trans. Magn.* **26** 2589
[108] Ren W J, Yang J L, Li B, Li D, Zhao X G and Zhang Z D 2009 *Physica B* **404** 3410
[109] Wang B W, Cheng L Z and He K Y 1996 *J. Appl. Phys.* **80** 6903
[110] Wang B W, Hao Y M, Busbridge S C, Guo Z J and Li Y X 2002 *J. Magn. Magn. Mater.* **246** 270
[111] Guo H Q, Gong H Y, Yang H Y, Li Y F, Yang L Y, Shen B G and Li R Q 1996 *Phys. Rev. B* **54** 4107
[112] Guo Z J, Zhang Z D, Wang B W and Zhao X G 2000 *Phys. Rev. B* **61** 3519
[113] Lv X K, Liu W, Yang F, Li J and Zhang Z D 2010 *J. Magn. Magn. Mater.* **322** 3173
[114] Guo Z J, Busbridge S C, Wang B W, Zhang Z D and Zhao X G 1999 *J. Appl. Phys.* **85** 6677
[115] Guo Z J, Zhang Z D, Zhao X G, Jin X M and Geng D Y 2000 *J. Alloys Compd.* **308** 319
[116] Guo Z J, Zhang Z D, Zhao X G, Liu W, Jin X M, Geng D Y, Lui J P and Busbridge S C 2001 *IEEE Trans. Magn.* **37** 2693
[117] Ma T Y, Yan M, Chen X Y, Jiang C B and Xu H B 2008 *Physica B* **403** 3677
[118] Mushnikov N V, Korolyov A V, Gaviko V S and Raevski Y I 1991 *J. Appl. Phys.* **70** 2768